1 **A feedback loop between heterochromatin and the nucleopore complex controls germ-**
2 **cell to oocyte transition during *Drosophila* oogenesis**
3

4 Kahini Sarkar[1], Noor M Kotb[1,2], Alex Lemus[1], Elliot T Martin[1], Alicia McCarthy[1,3], Justin
5 Camacho[1], Ayman Iqbal[1], Alex M. Valm[1], Morgan A Sammons[1], Prashanth Rangan[1*]
6
7 [1]Department of Biological Sciences/RNA Institute, University at Albany SUNY, Albany, NY
8 12222
9
10 [2]Department of Biomedical Sciences, The School of Public Health, University at Albany SUNY,
11 Albany, NY 12222
12
13 [3]Current address: 10x Genomics Headquarters, 6230 Stoneridge Mall Rd, Pleasanton, CA
14 94588
15
16
17 *Corresponding Author and Lead Contact: prangan@albany.edu
18

19 **Summary**
20

21 Germ cells differentiate into oocytes that become totipotent upon fertilization. How the highly
22 specialized oocyte acquires this distinct cell fate is poorly understood. During *Drosophila*
23 oogenesis, H3K9me3 histone methyltransferase SETDB1 translocates from the cytoplasm to the
24 nucleus of germ cells concurrent with oocyte specification. Here, we discovered that nuclear
25 SETDB1 is required to silence a cohort of differentiation-promoting genes by mediating their
26 heterochromatinization. Intriguingly, SETDB1 is also required for the upregulation of 18 of the ~30
27 nucleoporins (Nups) that comprise the nucleopore complex (NPC). NPCs in turn anchor SETDB1-
28 dependent heterochromatin at the nuclear periphery to maintain H3K9me3 and gene silencing in
29 the egg chambers. Aberrant gene expression due to loss of SETDB1 or Nups results in loss of
30 oocyte identity, cell death and sterility. Thus, a feedback loop between heterochromatin and NPCs
31 promotes transcriptional reprogramming at the onset of oocyte specification that is critical to
32 establish oocyte identity.
33

34 **Introduction**
35

36 Germ cells give rise to gametes that upon fertilization launch the next generation (Cinalli et al.,
37 2008; Seydoux and Braun, 2006; Spradling et al., 2011). In the gonad, germ cells become
38 germline stem cells (GSCs) that self-renew and differentiate to give rise to sperm or an oocyte
39 (Gilboa and Lehmann, 2004; Kershner et al., 2013; Ko et al., 2010; Lesch and Page, 2012; Reik
40 and Surani, 2015; Seydoux and Braun, 2006). The oocyte, upon fertilization or by
41 parthenogenesis, can differentiate into every cell lineage in the adult organism and thus has a
42 capacity to be totipotent (Ben-Ami and Heller, 2005; Lehmann, 2012; Riparbelli et al., 2017; Yuan
43 and Yamashita, 2010). The gene regulatory mechanisms that enable the transition from germ
44 cells to oocytes are not fully understood.

45

46   *Drosophila* has a well-characterized transition from germline stem cell (GSC) to an oocyte
47 (Dansereau and Lasko, 2008; Gilboa and Lehmann, 2004; Spradling et al., 2011; Allan C
48 Spradling, 1993). *Drosophila* ovaries comprise individual units called ovarioles that house the
49 GSCs in a structure called the germarium (**Figure 1A-A1**) (Lehmann, 2012; Xie and Spradling,
50 2000). GSC division results in a new GSC (self-renewal) and a cystoblast, which differentiates via
51 incomplete mitotic divisions, giving rise to 2-, 4-, 8- and 16-cell cysts (**Figure 1A1**) (Chen and
52 McKearin, 2003a, 2003b; Xie, 2013). One of these 16 cells is specified as the oocyte whereas
53 the other 15 cells become nurse cells (Huynh and St Johnston, 2004; Koch et al., 1967; Navarro
54 et al., 2004). Somatic cells envelop the nurse cells and the specified oocyte to form an egg
55 chamber (**Figure 1A1**) (Xie and Spradling, 2000). The nurse cells produce mRNAs, called
56 maternal mRNAs, that are deposited into the specified oocyte mediated by an RNA binding
57 protein, Egalitarian (Egl) (Blatt et al., 2020; Kugler and Lasko, 2009; Lilly and Spradling, 1996;
58 Mach and Lehmann, 1997; Navarro et al., 2004; A C Spradling, 1993). An inability to specify or
59 maintain the oocyte fate leads to death of the egg chamber mid-oogenesis and, in turn, sterility
60 (Blatt et al., 2021; Navarro et al., 2004).

61

62   The transition from GSC to an oocyte requires dynamic changes in gene expression that promote
63 progressive differentiation (Flora et al., 2017). Once a GSC gives rise to the cystoblast, it
64 expresses differentiation factor Bag of marbles (Bam), promoting its differentiation to an 8-cell
65 cyst (McKearin and Ohlstein, 1995; McKearin and Spradling, 1990). In the 8-cell cyst, the
66 expression of the RNA binding fox-1 homolog 1 (Rbfox1) is required to mediate transition into the
67 16-cell cyst stage, allowing for an oocyte to be specified (Carreira-Rosario et al., 2016).
68 Translation of Rbfox1 requires increased levels of ribosomal small subunit protein 19 (RpS19)
69 accomplished in part by expression of the germline specific paralog *RpS19b* in the
70 undifferentiated and early differentiating stages (McCarthy et al., 2019). During differentiation,
71 the germline also initiates meiotic recombination mediated by the synaptonemal complex
72 consisting of proteins such as Sisters Unbound (Sunn), Corona (Cona) and Orientation Disruptor
73 (Ord) (Ables, 2015; Cahoon and Hawley, 2016; Hughes et al., 2018; Orr-Weaver, 1995; Page and
74 Hawley, 2001). More than one cell in the cyst stage initiates recombination but as oocyte
75 differentiation proceeds, only the specified oocyte retains the synaptonemal complex (**Figure
76 1A1**) (Ables, 2015; Orr-Weaver, 1995; Page and Hawley, 2001). After oocyte-specification, the
77 levels of mRNAs encoding *RpS19b* and some synaptonemal complex proteins are diminished,
78 suggesting early oogenesis genes are no longer expressed (McCarthy et al., 2019). How the
79 expression of these early oogenesis genes is attenuated is not known.

80

81   In *Drosophila*, the <u>SET</u> <u>D</u>omain <u>B</u>ifurcated Histone Lysine Methyltransferase 1 (SETDB1) (also
82 called Eggless) is required for deposition of gene silencing Histone H3 Lysine 9 trimethylation
83 (H3K9me3) marks and heterochromatin formation (Clough et al., 2014, 2007; Rangan et al.,
84 2011; Yoon et al., 2008). SETDB1 is expressed throughout *Drosophila* oogenesis, but as the
85 oocyte is specified, it shifts from a cytoplasmic to predominantly nuclear localization (Clough et
86 al., 2007). A conserved cofactor called Windei (Wde) is required for either nuclear translocation,
87 nuclear stability, or targeting of SETDB1 to its target loci (Koch et al., 2009; Osumi et al., 2019).
88 Loss of *SETDB1* during germline development results in an accumulation of undifferentiated cells

89   (Rangan et al., 2011; Smolko et al., 2018). In addition, loss of *SETDB1* and *wde* also result in egg
90   chambers that do not grow in size and die mid-oogenesis (Clough et al., 2014; Koch et al., 2009).
91   *SETDB1* is known to be required for silencing transposons and male-specific transcripts in the
92   female germline (Czech et al., 2018; Rangan et al., 2011; Smolko et al., 2018). However, neither
93   the upregulation of transposons nor male-specific genes in female germline result in egg
94   chambers that do not grow in size (Malone et al., 2009; Shapiro-Kulnane et al., 2015; Smolko et
95   al., 2020). Together these data suggests that SETDB1 silences a yet-unidentified group of genes
96   to promote oogenesis.
97
98   Here, we find that genes that are expressed in early stages of oogenesis, including genes that
99   promote oocyte differentiation and synaptonemal complex formation, are silenced upon oocyte
100   specification, via a feedback loop between SETDB1-mediated heterochromatin and the
101   nucleopore complex (NPC). Inability to silence these differentiation-promoting genes due to loss
102   of either SETDB1 or members of the NPC results in loss of oocyte identity and death. Several
103   aspects of germ cell differentiation have been studied and have been implicated in loss of fertility
104   in sexually reproducing organisms. Our work indicates that a previously unappreciated broad
105   transcriptional reprogramming silences critical aspects of the germ cell differentiation program at
106   the onset of oocyte specification and is essential to promote oocyte identity.
107
108   **Results**
109
110   ***SETDB1* promotes silencing of *RpS19b* reporter at the onset of oocyte specification**
111   We hypothesized that the expression of early oogenesis mRNAs such as *RpS19b* is silenced
112   upon oocyte specification. To monitor *RpS19b* expression, we used a reporter that expresses an
113   RpS19b-GFP fusion from the endogenous *RpS19b* promoter. This RpS19b-GFP shows high
114   expression in the germarium and attenuated expression post-oocyte specification and in the
115   subsequent egg chambers, consistent with its endogenous *RpS19b* mRNA expression pattern
116   (**Figure 1B-C1, G**) (Jevitt et al., 2020; McCarthy et al., 2019).
117
118   Using a previously characterized hemagglutinin (HA) tagged endogenous SETDB1, we found that
119   a large fraction of SETDB1 translocates from the cytoplasm to the nucleus concurrent with oocyte
120   specification (**Figure S1A-A3**) (Seum et al., 2007). To test if *SETDB1* is required for the silencing
121   of *RpS19b* (Clough et al., 2014, 2007), we performed germline knockdown (GKD) of *SETDB1*, in
122   the background of *RpS19b-GFP* reporter. We detected the germline, RpS19b-GFP, and
123   spectrosomes/fusomes/somatic cell membrane in ovaries by immunostaining for Vasa, GFP, and
124   1B1, respectively (Lasko and Ashburner, 1988; Zaccai and Lipshitz, 1996). We found that,
125   compared to the control, GKD of *SETDB1* resulted in ectopic RpS19b-GFP protein expression in
126   the differentiated egg chambers without affecting levels in the undifferentiated stages (**Figure 1C-
127   G; Figure S1B**). Thus, *SETDB1* is required for repression of *RpS19b-GFP* reporter in the
128   differentiated egg chambers.
129
130   To determine if nuclear SETDB1 was required to repress *RpS19b-GFP* post-oocyte specification,
131   we depleted *wde* in the germline and independently assayed for SETDB1 nuclear localization,
132   H3K9me3, and RpS19b-GFP (**Figure S1C**). GKD of *wde* resulted in loss of nuclear SETDB1 in

133   the differentiated stages of oogenesis without affecting cytoplasmic levels in the undifferentiated
134   stages (**Figure S1D-F**). Whereas GKD of *SETDB1* reduced H3K9me3 throughout oogenesis,
135   GKD of *wde* reduced H3K9me3 only in the differentiated egg chambers but not in the
136   undifferentiated stages (**Figure S1G-J**). We found that GKD of *wde*, like GKD of *SETDB1*, results
137   in ectopic RpS19b-GFP protein expression in the egg chambers without affecting levels in the
138   undifferentiated stages (**Figure 1C-G**). In addition to upregulation of RpS19b-GFP, GKD of both
139   *SETDB1* and *wde* resulted in egg chambers that did not grow in size and died mid-oogenesis as
140   previously reported (**Figure S1K**) (Clough et al., 2014; Koch et al., 2009). Thus, repression of the
141   *RpS19b-GFP* reporter in the differentiated egg chambers requires nuclear SETDB1.
142
143   **SETDB1 and Wde repress genes that are primarily expressed prior to oocyte specification**
144   To determine if SETDB1 and Wde repress other differentiation-promoting genes in addition to
145   *RpS19b*, we performed RNA Sequencing (RNA-seq). We compared ovaries from *SETDB1-* and
146   *wde-* GKD flies to ovaries from wild-type (WT) flies, including young virgin flies which lack late-
147   stage egg chambers. Principal component analysis of the RNA-seq data revealed that *SETDB1*
148   and *wde* ovary transcriptomes closely resembles young virgin WT rather than adult WT (**Figure
149   S2A**). Using a 1.5-fold cut off (Fold Change (FC)≥|1.5|) and False Discovery Rate (FDR)<0.05,
150   we found that compared to young virgin WT control, 2316 genes were upregulated and 1972 were
151   downregulated in *SETDB1* GKD ovaries, and 1075 genes were upregulated and 442 were
152   downregulated in *wde*-GKD ovaries (**Figure 2A-B**) (**Supplemental Table 1)**. Moreover,
153   comparing *wde-* to *SETDB1-* GKD ovaries showed significant overlap of the upregulated (80%)
154   and downregulated (75%) transcripts, suggesting that *SETDB1* and *Wde* co-regulate a cohort of
155   genes during oogenesis (**Figure 2C; Figure S2B**).
156
157   SETDB1 and Wde are known to repress gene expression, thus we first focused on mRNAs with
158   increased levels in the GKD ovaries (Clough et al., 2014; Osumi et al., 2019). Gene Ontology
159   (GO) analysis of the shared upregulated RNAs indicated that many were genes involved in
160   differentiation (**Figure 2D**). Among the upregulated RNAs was *RpS19b*, validating our initial
161   screen, as well as genes that promote synaptonemal complex formation such as *sunn, ord* and
162   *cona* (**Figure 2E; Figure S2C-E**). In addition, the *blanks* mRNA, which is highly expressed only
163   in GSCs, cystoblasts and early cysts of WT, was upregulated and ectopically expressed in the
164   egg chambers of *SETDB1-* and *wde*-GKD ovaries (**Figure 2F; Figure S2F-I**) (Blatt et al., 2021).
165   Blanks is a component of a nuclear siRNA pathway that has critical roles in the testis but does
166   not have any overt function during oogenesis (Gerbasi et al., 2011). Thus, *SETDB1* and *wde*
167   repress a cohort of RNAs that are either critical for transition from GSC to an oocyte or merely
168   expressed during early oogenesis.
169
170   To determine when during oogenesis SETDB1 and Wde act to repress genes, we analyzed
171   available RNA-seq libraries that were enriched for GSCs, cystoblasts, and cysts, early egg
172   chambers and late-stage egg chambers (McCarthy et al., 2019). We found that *SETDB1/wde*-
173   regulated RNAs decreased after the cyst stages and their levels were attenuated in the later
174   stages of oogenesis compared to non-targets (**Figure 2G, Figure S2J-L**) (McCarthy et al., 2019).
175   This reduction did not happen in absence of *SETDB1* and *wde* (**Figure 2G**). RNA *in situ* analysis
176   of *blanks*, and *RpS19b* revealed that these mRNAs are present in the early stages of oogenesis

177 and are attenuated after oocyte specification in controls but that these RNAs persisted in *SETDB1*
178 and *wde* GKD egg chambers (**Figure 2H-O**). Thus, mRNAs that are broadly expressed prior to
179 oocyte specification, become repressed by SETDB1 and Wde in differentiated egg chambers.
180
181 **SETDB1 represses transcription of a subset of targets by increasing H3K9me3 enrichment**
182 To investigate whether SETDB1/Wde-regulated mRNAs are repressed at the level of
183 transcription, we examined a subset of nascent mRNAs (pre-mRNAs) by qRT-PCR. Indeed, the
184 levels of nascent *RpS19b*, *ord*, *sunn*, *cona* and *blanks* mRNAs were increased in *SETDB1*/*wde*-
185 GKDs ovaries compared to control WT ovaries (**Figure S3A-B**). These data suggest that
186 transcription of these genes increases upon loss of SETDB1 or Wde.
187
188 To determine if the SETDB1-dependent repression of these genes involves changes in H3K9me3,
189 we performed CUT&RUN (Ahmad, 2018; Skene and Henikoff, 2017) on adult WT ovaries
190 enriched for differentiated egg chambers where these genes are repressed (**Figure 2G**). Analysis
191 of CUT& RUN data from adult WT showed enrichment of H3K9me3 marks on previously identified
192 SETDB1 targets and genes containing heterochromatin such as PHD Finger Protein 7 (*phf7)* and
193 *light* (*lt)* respectively validating our CUT&RUN data (**Figure 3A-B; Figure S3C)** (Devlin et al.,
194 1990; Smolko et al., 2018). As genes in *Drosophila* genome are closely packed, we only analyzed
195 the gene body from 5'UTR to the end of the 3'UTR to unambiguously identify SETDB1 regulated
196 genes (Schwartz and Cavalli, 2017). We found that 1593 out of 2,316 genes upregulated upon
197 loss of SETDB1 are enriched for H3K9me3 marks compared to IgG negative control (**Figure 3C**).
198 In addition, we found that 888 genes lose H3K9me3 on their gene bodies upon GKD of *SETDB1*
199 including *RpS19b* and ATP-dependent chromatin assembly factor (*Acf)* (**Figure 3D-F**). The
200 upregulated genes that do not show changes to H3K9me3 marks within the gene body may be
201 regulated by elements outside of the gene body or indirectly. Importantly, taken together, our data
202 suggest that SETDB1 is required for H3K9me3 enrichment and transcriptional repression of a
203 cohort of early-oogenesis genes in the egg chamber.
204
205 *SETDB1* is required for transposon repression during oogenesis (Andersen et al., 2017; Rangan
206 et al., 2011), and the upregulation of transposons can affect gene expression (Sienski et al., 2012;
207 Upadhyay et al., 2016). However, we found that the upregulation of genes in the differentiated
208 stages that we observed upon depletion of *SETDB1* was not due to the secondary effect of
209 transposon upregulation as the expression of *RpS19b* reporter was not altered in germline
210 depleted of *aubergine* (*aub*), a critical component of the piRNA pathway (**Figure S3D-F**) (Chen
211 et al., 2007; Czech et al., 2018; Malone et al., 2009; Wang et al., 2015). Nor, did *aub* depletion
212 cause mid-oogenesis death as we observed in *SETDB1* and *wde* GKDs (**Figure S3D-F**) (Chen
213 et al., 2007; Wilson et al., 1996). Overall, our data suggest that loss of *SETDB1* derepresses a
214 subset of genes during late oogenesis via decreased H3K9me3, independent of transposon
215 dysregulation.
216
217 **SETDB1 is required for the expression of NPC components**
218 GO term analysis of downregulated targets of *SETDB1*/*wde* GKD included genes that regulate
219 transposition, consistent with the previously described role of SETDB1/Wde in the piRNA pathway
220 and those that regulate proper oocyte development, consistent with the previously described

221 phenotype (**Figure 4A**)(Andersen et al., 2017; Clough et al., 2007; Koch et al., 2009; Rangan et
222 al., 2011).
223

224 Unexpectedly, we observed that genes involved in nucleocytoplasmic transport were
225 downregulated in *SETDB1/wde*-GKD ovaries as compared to controls (**Figure 4A**).
226 Nucleocytoplasmic transport is mediated by Nucleopore complexes (NPCs), which span the
227 nuclear membrane and consist of a cytoplasmic ring, a central scaffold spanning the nuclear
228 envelope, and a nuclear ring and basket (**Figure 4B**) (M. Capelson et al., 2010; Doucet and
229 Hetzer, 2010; Gozalo and Capelson, 2016). Beyond regulating nucleocytoplasmic transport,
230 NPCs also regulate gene transcription, for instance by anchoring and maintaining
231 heterochromatic domains (Capelson and Hetzer, 2009; Hou and Corces, 2010; Iglesias et al.,
232 2020; Sarma and Willis, 2012; Sood and Brickner, 2014). We found that GKD of *SETDB1/wde* in
233 the germline resulted in downregulation of 18 out of ~30 nucleoporins (Nups) that make up the
234 Nucleopore complex in *Drosophila* (**Figure 4C**), including a germline enriched *Nup154* that is
235 critical for oogenesis (Colozza et al., 2011; Gigliotti et al., 1998; Grimaldi et al., 2007). The Nups
236 that were downregulated upon depletion of *SETDB1* and *wde* were not isolated to one specific
237 NPC subcomplex (**Figure 4B-C**).
238

239 We found that nascent mRNAs corresponding to the *SETDB1/Wde* targets *Nup154*, *Nup205* and
240 *Nup107* were downregulated in *SETDB1/wde*-GKD ovaries, whereas the non-target *Nup62* was
241 unaffected, suggesting that SETDB1/Wde promotes transcription of a cohort of *Nups* (**Figure 4D**).
242 In addition, the levels of a Nup107-RFP fusion protein, under endogenous control (Katsani et al.,
243 2008), were significantly reduced in the cysts and egg chambers of *SETDB1*- and *wde*-GKD
244 compared to controls (**Figure S4A-D**).
245

246 To determine if loss of *Nup* expression in *SETDB1/wde*-GKD ovaries resulted in loss of NPC
247 formation, we performed immunofluorescence with an antibody that is known to mark NPCs in
248 *Drosophila* (Maya Capelson et al., 2010; Davis and Blobel, 1987; Hampoelz et al., 2019; Kuhn et
249 al., 2019). We found that NPC levels were reduced in the egg chambers of *SETDB1/wde*-GKD
250 ovaries compared to controls (**Figure 4E-H**), but the nuclear lamina was unaffected (**Figure S4E-
251 H**), and NPCs in the soma were also unaffected (**Figure 4I**). Thus, *SETDB1/wde* are required for
252 the proper expression of Nups and NPC formation after oocyte specification.
253

254 Heterochromatic genes and piRNA clusters require heterochromatin to promote their transcription
255 (Rangan et al., 2011; Weiler and Wakimoto, 1995). Although we found that *SETDB1* is required
256 for upregulation of Nups, CUT&RUN analysis of H3K9me3 marks revealed that only 3 of the *Nup*
257 genes had any enrichment of H3K9me3 (*Mbo*, *Nup188*, *Gp210*). Moreover, among *SETDB1*-
258 regulated *Nups*, only Gp210 showed any heterochromatic enrichment **(Supplemental Table 2).**
259 Taken together, we find that *SETDB1* promotes proper expression of *Nups* by a yet unknown
260 mechanism in the germline.
261

262 **Nucleoporins are required to maintain heterochromatin domains at the nuclear periphery**
263 Our data so far indicate that, in *Drosophila* female germline, heterochromatin formation mediated
264 by SETDB1 is required for proper NPC formation by promoting proper expression of a subset of

Nups including *Nup107* and *Nup154* (**Figure 4C**). In yeast, a subset of Nups are part of the heterochromatin proteome and are required to cluster and maintain heterochromatin at the NPC (Iglesias et al., 2020). This subset includes Nup107 and the yeast homolog of Nup154, Nup155, which both have reduced expression in *SETDB1/Wde*-GKD compared to controls. We hypothesized that in *Drosophila,* SETDB1 could promote silencing of early oogenesis genes by promoting heterochromatin formation. This heterochromatin then promotes expression of Nups and NPC formation, which can then help maintain heterochromatin by anchoring it to nuclear periphery and thus promoting silencing of early-oogenesis genes.

To first determine if heterochromatin and nucleoporins associate in *Drosophila* female germline, we utilized antibody against H3K9me3 to mark heterochromatin and Nup107-RFP to mark NPCs in WT ovarioles (Katsani et al., 2008; Rangan et al., 2011). We found that H3K9me3 domains were often at the nuclear periphery, in close proximity with Nup107-RFP (**Figure 5A-A2, E**). Next, to determine if loss of *Nups* leads to loss of heterochromatin, we first depleted *Nup154* and probed for heterochromatin formation. We chose *Nup154*, as its loss of function phenotype of *Nup154* has been well described (Gigliotti et al., 1998; Grimaldi et al., 2007). We found that GKD of *Nup154* in the germline, resulted in egg chambers that do not grow and die mid-oogenesis as previously described for *Nup154* mutants **(Figure S5A-B2)** (Gigliotti et al., 1998). In addition, depletion of *Nup154* results in proper translocation of SETDB1 from the cytoplasm to the nucleus suggesting that transport of SETDB1 into the nucleus is not grossly affected **(Figure S5C-D1)**. By staining for H3K9me3 marks, we found that upon GKD of *Nup154*, heterochromatin domains initially form (**Figure S5E-F2**). However, in the egg chambers of *Nup 154* GKD, the colocalization between H3K9me3 domains and Nup107-RFP levels at the nuclear periphery were significantly reduced prior to significant reduction of heterochromatin levels **(Figure 5A-D1, Figure S5E-F3, I)**. GKD of *Nup107* also resulted in egg chambers that do not grow and loss of heterochromatin **(Figure S5E-I)**. Thus, *Nups 154* and *107,* which are positively regulated by *SETDB1*, are required for H3K9me3 localization at the nuclear periphery for H3K9me3 maintenance in the female germline.

Nups are required for silencing early-oogenesis genes

Based on our findings above that Nups are required to maintain H3K9me3 levels and localization, we hypothesized that they are also required to silence the early-oogenesis RNAs in differentiated egg chambers. To test this hypothesis, we depleted *Nup154* and *Nup107* in the germline of a fly carrying the *RpS19b-GFP* reporter. We found that GKD of these nucleoporins resulted in upregulation of RpS19b-GFP phenocopying GKD of *SETDB1/wde* (**Figure 6A-C; Figure S6A-B1, D**). Moreover, germline depletion of *Nup62,* which is within the NPC but not regulated by SETDB1, also resulted in upregulation of *RpS19bGFP* and egg chambers that did not grow (**Figure S6A-D**). This suggests that activity of NPC components and not just the Nups regulated by SETDB1 are required for silencing *RpS19b-GFP* reporter.

To determine if Nups are required for silencing other early oogenesis RNAs, we performed RNA-seq, and compared *Nup154* GKD ovaries with young ovaries as a developmental control **(Figure S2A)**. Using a 1.5-fold cut off (Fold Change (FC)≥|1.5|) and False discovery rate (FDR)<0.05), we found that compared to control, in *Nup154* GKD 2809 genes are upregulated, and 2922 genes

7

309   are downregulated (**Figure 6D) (Supplemental Table 1)**. Strikingly, 97% of upregulated genes
310   and 89% of downregulated *SETDB1/Wde* targets overlapped with *Nup154* GKD (**Figure 6E;**
311   **S6E**). *Nup154* was involved in silencing genes that promote oocyte differentiation including
312   synaptonemal complex components *ord*, *sunn* and *cona* as well as *RpS19b* (**Figure 6F; S6F-H**).
313   In addition, GKD of *Nup154* also resulted in upregulation of *blanks* (**Figure 6G**). The levels of
314   *Nup154*-regulated RNAs decreased after the cyst stage, when the oocyte is specified, in contrast
315   to non-targets, which have similar RNA levels at all stages (**Figure 6H; S6I-J**). Thus, Nup154 is
316   critical for silencing early-oogenic mRNAs in the differentiated egg chambers.
317
318   To determine if *Nup154* is required for H3K9me3 marks at SETDB1-regulated gene, loci such as
319   *RpS19b*, we carried out CUT& RUN for H3K9me3 in control and *Nup154* GKD. We found that
320   564 out of 622 genes displaying a loss in H3K9me3 in Nup154 GKD also show the same loss in
321   *SETDB1* GKD including *RpS19b* and *Acf* (**Figure 6I; S6K-L**) (**Supplemental Table 2**). Taken
322   together, we find that Nups are required for silencing and H3K9me3 at a subset of *SETDB1/Wde*-
323   regulated loci.
324
325   **Silencing genes expressed during the early oogenesis stages is required for maintaining**
326   **oocyte fate**
327   We next asked why loss of *SETDB1, wde* and *Nups* results in egg chambers that do not grow
328   and die mid-oogenesis. Egg chambers with oocyte specification or maintenance defects result in
329   death of egg chambers mid-oogenesis (Blatt et al., 2021). To determine if there are oocyte
330   specification or maintenance defects, we stained GKD of *SETDB1, wde* and *Nup154* for the
331   oocyte marker Egalitarian (Egl) as well as Vasa and 1B1 (Mach and Lehmann, 1997; Navarro et
332   al., 2004). In the early stages of oogenesis, as in control, GKD of *SETDB1, wde* and *Nup154*
333   resulted in one Egl positive cell, suggesting that oocyte is specified (**Figure 7A-E**). While initial
334   Egl localization to oocytes appeared to be normal, we cannot rule out subtle specification defects.
335   However, in the later egg chambers, compared to control ovariole, GKD of *SETDB1, wde* and
336   *Nup154* resulted in either mis-localization or diffuse Egl expression suggesting loss of oocyte fate
337   (**Figure 7A-E**). Taken together, these data suggest that SETDB1, Wde and Nup154 are required
338   for maintaining the oocyte fate.
339
340   **Discussion**
341
342   Many maternally contributed mRNAs in oocytes are critical for early development after fertilization
343   (Calvi et al., 1998; Huynh and St Johnston, 2004; Kugler and Lasko, 2009; Navarro et al., 2004;
344   Telfer, 1975). We previously showed that many mRNAs expressed in germ cells and the
345   undifferentiated stages of oogenesis must be selectively degraded and thus excluded from the
346   maternal contribution (Blatt et al., 2021). However, the potential role of transcriptional silencing
347   of germ cell and GSC-enriched genes during oogenesis was unclear. Here, we found that
348   regulated translocation of SETDB1 into the nucleus during oocyte specification is required to
349   silence germ cell- and early oogenesis-genes in the differentiated egg chambers (**Figure 7F**), and
350   that this process is essential to maintain oocyte fate. Thus, some genes that are expressed in
351   germ cells and some that promote differentiation are transcriptionally silenced at the onset of
352   oocyte specification mediated by a feedback loop between heterochromatin and NPC.

8

353

Regulated heterochromatin formation during oocyte specification promotes germ cell to oocyte transition

A large fraction of SETDB1 is cytoplasmic in the undifferentiated stages of the germline. As the oocyte is being specified during differentiation, SETDB1 becomes mostly nuclear (Clough et al., 2014). This translocation of SETDB1 to the nucleus during oocyte specification is mediated by Windei (Wde), the *Drosophila* ortholog of mAM/MCAF1 (Koch et al., 2009; Osumi et al., 2019). Here we find that translocation of SETDB1 to the nucleus during oocyte specification is required to silence germ cell and early-oogenesis genes at the onset of oocyte specification. MCAF1 also regulates the accumulation of SETDB1 in the nucleus in mammalian cells (Tsusaka et al., 2019). In addition, loss of *SETDB1* during mammalian oogenesis results in meiotic defects and infertility (Eymery et al., 2016). These data suggest that regulated heterochromatin formation is conserved to promote proper oogenesis in mammals.

We discovered that SETDB1 is required to silence two major classes of genes. The first group is involved in GSC differentiation into an oocyte, including critical genes that promote meiosis I. The second group of genes are those that are merely expressed in the germ cells prior to differentiation into an oocyte, but have no specific function in the female germline such as *blanks* (Blatt et al., 2021; Gerbasi et al., 2011). We propose that these genes that are silenced upon oocyte specification are either detrimental to late oogenesis or early embryogenesis. Indeed, it has been shown that overexpression of one such gene *actin 57B* (*act57B),* which is repressed by SETDB1/Wde **(Supplemental Table 1)**, is detrimental to oogenesis (Blatt et al., 2021; Duan et al., 2020). Remarkably, some of the mRNAs encoded by genes that are transcriptionally silenced by SETDB1 during this transition are also targeted at the post-transcriptional level for degradation by members of the no go decay pathway such as *blanks* and *Act57B* (Blatt et al., 2021). Thus, our data suggests that the regulation of gene expression during the germ cell to oocyte transition reflects a two-step process: transcriptional silencing dependent on SETDB1, and post-transcriptional degradation of mRNAs to exclude a cohort of germ cell mRNAs from the maternal contribution (Blatt et al., 2021).

SETDB1 is guided to its target transposons and piRNA clusters mediated by piRNAs (Andersen et al., 2017; Czech et al., 2018; Koch et al., 2009; Osumi et al., 2019). However, our data suggests that the piRNA pathway does not play a part in silencing germ cell and early oogenesis RNAs. We find that loss of *aub* does not result in upregulation of *RpS19b*. This result is consistent with the fact that loss of *aub* and *piwi* in the germline does not result in egg chambers that do not grow (Chen et al., 2007; Wilson et al., 1996). In somatic cells of the gonad, loss of *wde* function eliminates nuclear SETDB1 signal (Osumi et al., 2019; Timms et al., 2016). However, upon depletion of Wde, SETDB1 was still ubiquitinated, a requirement for its nuclear retention (Osumi et al., 2019). This suggests that in absence of Wde, SETDB1 can translocate to the nucleus but cannot find its targets. Osumi *et al.* (2019) suggested that Wde could mediate SETDB1 recruitment to the its targets, leading to H3K9me3 deposition. In mammals, it has been shown that transcriptional factors such as the KRAB domain-containing Zinc finger proteins recruit SETDB1 to the target genes for silencing, but such transcription factors have not been identified in the female gonad (Frietze et al., 2010; Schultz et al., 2002). Thus, SETDB1 targets germ cell

397 and early oogenesis genes for silencing independent of the piRNA pathway but through a yet
398 undetermined mechanism, either through Wde or through yet undetermined transcription factors.
399

**400 Nucleopore complex and heterochromatin are in a feedback loop to promote gene
401 silencing**
402 The NPC not only mediates selective nucleo-cytoplasmic transport of macromolecules but also
403 regulates gene expression by anchoring chromatin domains, including heterochromatin to the
404 nuclear periphery (Maya Capelson et al., 2010; M. Capelson et al., 2010; Holla et al., 2020;
405 Iglesias et al., 2020; Sarma and Willis, 2012). In addition, in yeast, several Nups are also part of
406 the heterochromatin proteome suggesting that NPCs can regulate gene expression by regulating
407 heterochromatin (Brickner et al., 2019; Iglesias et al., 2020). Consistent with these observations,
408 we find that in the female germline of *Drosophila*, NPC and heterochromatin are closely
409 associated. Loss of NPCs due to depletion of individual Nups results in loss of heterochromatin
410 and subsequent upregulation of germ cell and early oogenesis genes resulting in oogenesis
411 defects. The 97% overlap of target genes between *SETDB1*, *wde* and *Nup154* is indicative that
412 Nups are functioning in the same pathway as SETDB1. This suggests that in the female germline,
413 not only do NPCs associate with heterochromatin, but that NPCs also play a role in maintaining
414 heterochromatin and gene repression during germ cell to oocyte transition.
415

416 Silencing of early oogenesis genes at the onset of oocyte specification is timed with exit from
417 mitotic cell cycle. *Drosophila* nucleopore complex consists of ~30 different nucleoporins some of
418 which are solubilized during early mitotic cell division (Güttinger et al., 2009; Laurell and Kutay,
419 2011). Nucleoporins are recruited to the chromatin in early anaphase followed by sequential
420 reassembly of the complex (Kiseleva et al., 2001; Kutay et al., 2021). During *Drosophila*
421 oogenesis, in the premeiotic stage, the GSC divides to eventually produce a 16-cell cyst (Huynh
422 and St Johnston, 2004; Koch et al., 1967; Lehmann, 2012; Spradling et al., 2011). Prophase-I of
423 meiosis begins in cysts where the oocyte is also specified (Ables, 2015; Orr-Weaver, 1995). We
424 find that nucleoporins promote silencing of genes that are required for initiation of meiosis I such
425 as *Rbfox1* and synaptonemal complex components *ord*, *sunn* and *cona* once the cysts have
426 stopped dividing and the oocyte is being specified. Taken together, our data suggests a
427 mechanism wherein after the mitotic division of cysts have ceased and meiosis I is initiated, the
428 reassembly of NPC simultaneously promotes silencing of the genes required for the transition
429 from mitotic GSC division to meiotic oocyte specification.
430

431 While NPC association with heterochromatin has been described, remarkably we find that loss of
432 heterochromatin results in attenuated expression of some but not all Nup mRNAs.
433 Heterochromatic genes and piRNA clusters require heterochromatin to promote their transcription
434 (Andersen et al., 2017; Devlin et al., 1990; Rangan et al., 2011). However, by analyzing CUT
435 &RUN data and previously published ChIP data of H3K9me3 marks, we found that only one Nup
436 regulated by SETDB1 is enriched for H3K9me3 marks. Therefore, SETDB1 indirectly promotes
437 expression of Nups.
438

439 The number of genes that need to be silenced varies based on cell types and developmental
440 trajectory. How levels of heterochromatin are coupled to their NPC docking sites in the cell was

441 not known. Like heterochromatin levels, the number of NPCs also varies by cell type and during
442 differentiation (McCloskey et al., 2018). How NPC number is regulated during development was
443 not fully understood. Our findings in the female germline suggest an elegant tuning mechanism
444 for heterochromatin and its NPC docking sites. Heterochromatin promotes levels of NPC which
445 then promote heterochromatin maintenance by tethering it to the nuclear periphery. We find that
446 this loop can be developmentally regulated by controlling levels of SETDB1 in the nucleus
447 mediated by conserved protein Wde to promote heterochromatin formation.
448
449 **Acknowledgements:**
450
460

461 **Materials and Methods**
462
463 **Fly lines**
464
465 The following RNAi stocks were used in this study; if more than one line is listed, then both were
466 quantitated and the first was shown in the main figure: *SETDB1* RNAi (Perrimon lab, (Rangan et
467 al., 2011), *Wde* RNAi (Bloomington #33339), *Nup154* RNAi (Bloomington #34710), *Nup93* RNAi
468 (VDRC #V16189), *Nup62* RNAi (Bloomington #35695), *Nup107* RNAi (Bloomington #43189),
469 *Nup205* RNAi (VDRC #V38608).

470 The following tagged lines were used in this study: *dSETDB1-HA* (Bontron Lab) (Seum et al.,
471 2007), *RpS19b-GFP* (Buszczak Lab, (McCarthy et al., 2019), mRFP-Nup107 (Bloomington
472 #35516).

473 The following tissue-specific drivers and double balancer lines were used in this study: *UAS-*
474 *Dcr2;nosGAL4* (Bloomington #25751), *nosGAL4;MKRS*/TM6 (Bloomington #4442), and
475 *If*/CyO*;nosGAL4* (Lehmann Lab).

476 **Reagents for fly husbandry**

477 Flies were grown at 25-29°C and dissected between 0-3 days post-eclosion.

478   Fly food was made using the procedures as previously described (summer/winter mix) and narrow
479   vials (Fisherbrand Drosophila Vials; Fischer Scientific) were filled to approximately 10-12mL
480   (Flora et al., 2018).

Dissection and Immunostaining

482   Ovaries were dissected and teased apart with mounting needles in cold PBS and kept on ice. All
483   incubation was done with nutation. Samples were fixed for 10 minutes in 5% methanol-free
484   formaldehyde. Ovaries were washed in 0.5 mL PBT (1X PBS, 0.5% Triton X-100, 0.3% BSA) 4
485   times for 5 minutes each. Primary antibodies in PBT were added and incubated at 4°C nutating
486   overnight. Samples were next washed 3 times for 5 minutes each in 0.5 mL PBT, and once in 0.5
487   mL PBT with 2% donkey serum (Sigma) for 15 minutes. Secondary antibodies were added in PBT
488   with 4% donkey serum and incubated at room temperature for 3-4 hours. Samples were washed
489   3 times for 10 minutes each in 0.5 mL of 1X PBST (0.2% Tween 20 in 1x PBS) and incubated in
490   Vectashield with DAPI (Vector Laboratories) for 1 hour before mounting.

491   The following primary antibodies were used: mouse anti-1B1 (1:20; DSHB), Rabbit anti-Vasa
492   (1:1,000; Rangan Lab), Chicken anti-Vasa (1:1,000; Rangan Lab) (Upadhyay et al., 2016), Rabbit
493   anti-GFP (1:2,000; abcam, ab6556), Rabbit anti-H3K9me3 (1:500; Active Motif, AB_2532132),
494   Mouse anti-H3K27me3 (1:500; abcam, ab6002), Rabbit anti-Egl (1:1,000; Lehmann Lab), Mouse
495   anti-NPC (1:2000; BioLegend, AB_2565026) and Rat anti-HA (1:500; Roche, 11 867 423 001).
496   The following secondary antibodies were used: Alexa 488 (Molecular Probes), Cy3 and Cy5
497   (Jackson Labs) were used at a dilution of 1:500.

Fluorescence Imaging

499   The tissues were visualized, and images were acquired using a Zeiss LSM-710 confocal
500   microscope under 20X, 40X and 63X oil objective with pinhole set to 1 airy unit. All gain, laser
501   power, and other relevant settings were kept constant for any immunostainings being compared.
502   Image processing was done using Fiji and gain adjustment and cropping was performed in
503   Photoshop CC 2019.

504
Colocalization analysis
506
507   Confocal images of control and Nup154-RNAi mutants labeled for RFP-Nup107, H3K9me3, and
508   DAPI were imported into Bitplane Imaris 9.6.2 for 3D reconstruction and colocalization analysis.
509   Colocalization between RFP-Nup107 and H3K9me3 was calculated on a per egg chamber basis
510   using the Surface-surface coloc function of Imaris and an automatic threshold detection and the
511   surface-to-surface coloc function. The number of colocalized voxels was then normalized to the
512   number of H3K9me3 voxels (Valm et al., 2017).

Egg laying assays

514   Assays were conducted in vials with 3 control or experimental females under testing and 1 wild
515   type control males. Crosses were set up in triplicate for both control and experimental. All flies
516   were 1-day old post-eclosion upon setting up the experiment. Cages were maintained at 29°C
517   and plates were changed daily for counting. Analyses were performed for 5 consecutive days.
518   Number of eggs laid were counted and averaged. Adult flies eclosed were counted from all the
519   vials and averaged.

520   **RNA isolation**

521   Ovaries from flies were dissected in cold 1x PBS. RNA was isolated using TRIzol (Invitrogen,
522   15596026) (Blatt et al., 2021; McCarthy et al., 2019).

523   RNA was treated with DNase (TURBO DNA-free Kit, Life Technologies, AM1907), and then run
524   on a 1% agarose gel to check integrity of the RNA.

525   **RNA-seq library preparation and analysis**

526   Libraries were prepared using the Biooscientific kit. To generate mRNA enriched libraries, total
527   RNA was treated with poly(A)tail selection beads (Bioo Scientific Corp., NOVA-512991).
528   Manufacturer's instructions of the NEXTflex Rapid Directional RNA-seq Kit (Bioo Scientific Corp.,
529   NOVA-5138-08) were followed, but RNA was fragmented for 13 minutes. Library quality was
530   assessed with a Fragment Analyzer (5200 Fragment Analyzer System, AATI, Ankeny, IA, USA)
531   following manufacturer's instructions. Single-end mRNA sequencing (75 base pair reads) was
532   performed on biological duplicates from each genotype on an Illumina NextSeq500 by the Center
533   for Functional Genomics (CFG).

534   After quality assessment, the sequenced reads were aligned to the *Drosophila melanogaster*
535   genome (UCSCdm6) using HISAT2 (version 2.1.0) with the RefSeq-annotated transcripts as a
536   guide (Kim et al., 2015). Differential gene expression was assayed by DeSeq2, using a false
537   discovery rate (FDR) of 0.05, and genes with 2-fold or higher were considered significant. The
538   raw and unprocessed data for RNA-seq generated during this study are available at Gene
539   Expression Omnibus (GEO) databank under accession number: XXX. GO term enrichment on
540   differentially expressed genes was performed using Panther (Thomas et al., 2006).

541   **Fluorescent *in situ* hybridization**

542   A modified *in situ* hybridization procedure for *Drosophila* ovaries was followed. Probes were
543   designed and generated by LGC Biosearch Technologies using Stellaris® RNA FISH Probe
544   Designer, with specificity to target base pairs of target mRNAs. Ovaries (3 pairs per sample) were
545   dissected in RNase free 1X PBS and fixed in 1 mL of 5% formaldehyde for 10 minutes. The
546   samples were then permeabilized in 1mL of Permeabilization Solution (PBST+1% Triton-X)
547   rotating in RT for 1 hour. Samples were then washed in wash buffer for 5 minutes (10% deionized
548   formamide and 10% 20x SSC in RNase-free water). Ovaries were covered and incubated
549   overnight with 1ul of probe in hybridization solution (10% dextran sulfate, 1 mg/ml yeast tRNA, 2

13

550   mM RNaseOUT, 0.02 mg/ml BSA, 5x SSC, 10% deionized formamide, and RNase-free water) at
551   30°C. Samples were then washed 2 times in 1 mL wash buffer for 30 minutes and mounted in
552   Vectashield.

CUT&RUN assay

554   Ovaries from flies were dissected in ice cold 1x PBS and ovarioles were separated by teasing
555   after dissection with mounting needles. PBS was removed and the samples were permeabilized
556   in 1mL of Permeabilization Solution (PBST+1% Triton-X) rotating in RT for 1 hour. Samples were
557   then incubated overnight at 4°C in primary antibody dilutions in freshly prepared BBT+ buffer
558   (PBST + 1% BSA + 0.5 mM Spermidine + 2 mM EDTA + 1 large Roche complete EDTA-free
559   tablets). Primary antibody was replaced with BBT+ buffer and quickly washed twice. Samples
560   were then incubated in ~700 ng/ml of pAG-MNase in BBT+ buffer rotating for 4 hours at 25°C.
561   Samples were then quickly washed twice in wash+ buffer (20 mM HEPES pH7.5 + 150 mM NaCl
562   + 0.1% BSA + 0.5 mM Spermidine + 1 large Roche complete EDTA-free tablets in water).
563   Samples were resuspended in 150 µl Wash+C (wash+ + 100 mM CaCl$_2$) and incubated for 45
564   minutes on nutator at 4°C. The cleavage reaction was terminated by addition of 150 µl StopR
565   (NaCl final 200 mM + EDTA final 20 mM + 100µg/mL RNaseA) and incubating the sample at 37˚C
566   for 30 minutes. Samples were then centrifuged at 16,000 x g for 5 minutes and 300 µl of the
567   supernatant was collected for DNA discovery. To the supernatant, 2 µL 10% SDS and 2.5 µL of
568   20 mg /mL Proteinase K was added and incubated at 50°C for 2 hours. Half of this was kept as a
569   backup and half was used in bead cleanup. 20 µL AmpureXP bead slurry and 280 µL MXP buffer
570   (20% PEG8000 + 2.5 M NaCl + 10 mM MgCl2 in water) was added to the sample and mixed
571   thoroughly followed by 15 minutes incubation at RT. The beads were separated by magnet and
572   supernatant was discarded. The beads were carefully washed with 80% ethanol for 30 seconds,
573   while on the magnetic stand and air dried for 2 minutes. The beads were then resuspended in 10
574   µL DNase free water.

DNA seq library preparation and analysis

576   The samples from CUT&RUN assay were used for library preparation using NEBNext® Ultra™
577   DNA Library Prep Kit for Illumina® (E7645, E7103) and adaptor ligated DNA were prepared
578   without size selection.

CUT&Run Data Analysis

580   Cut&Run libraries were sequenced as paired-end 75bp reads on the Illumina NextSeq 500 at the
581   University at Albany Center for Functional Genomics. FASTQ files were aligned to the dm6
582   reference genome using HISAT2 (10.1038/s41587-019-0201-4) (-X 10 -I 1000 –no-spliced-
583   alignment, --no-discordant). Mapping statistics and data will be available from Gene Expression
584   Omnibus. Alignment files were sorted and indexed using samtools and were subsequently used
585   to create bigwig files for visualization with deeptools (--binSize 10)(10.1093/nar/gkw257).
586   Principle component analysis between samples was performed using the multiBigwigSummary
587   and plotPCA modules from deeptools. Only gene bodies were considered and problematic

14

588   genomic regions (blacklist) were removed from the analysis (10.1038/s41598-019-45839-z). Raw
589   read counts of H3K9me3 enrichment across gene bodies was calculated using the HOMER
590   annotateRepeats function and differential enrichment was calculated using DESeq2 (HOMER
591   PMID:20513432, DESeq2 citation 10.1186/s13059-014-0550-8). H3K9me3 occupied genes are
592   those with differential enrichment of H3K9me3 compared to IgG matched control conditions using
593   DESeq2.

594   **Quantitative Real Time-PCR (qRT-PCR)**

595   1 µL of cDNA from each genotype was amplified using 5µL of SYBR green Master Mix, 0.3 µL of
596   10µM of each reverse and forward primers in a 10 µL reaction. The thermal cycling conditions
597   consisted of 50°C for 2 minutes, 95°C for 10 minutes, 40 cycles at 95°C for 15 seconds, and 60°C
598   for 60 seconds. The experiments were carried out in technical triplicate and minimum 2 biological
599   replicates for each sample. To calculate fold change in mRNA levels, comparison was done to
600   rp49 mRNA levels which was used as the control gene. Average of the $2^{\Delta Ct}$ for the biological
601   replicates was calculated. Error bars were plotted using standard error of the ratios and P-value
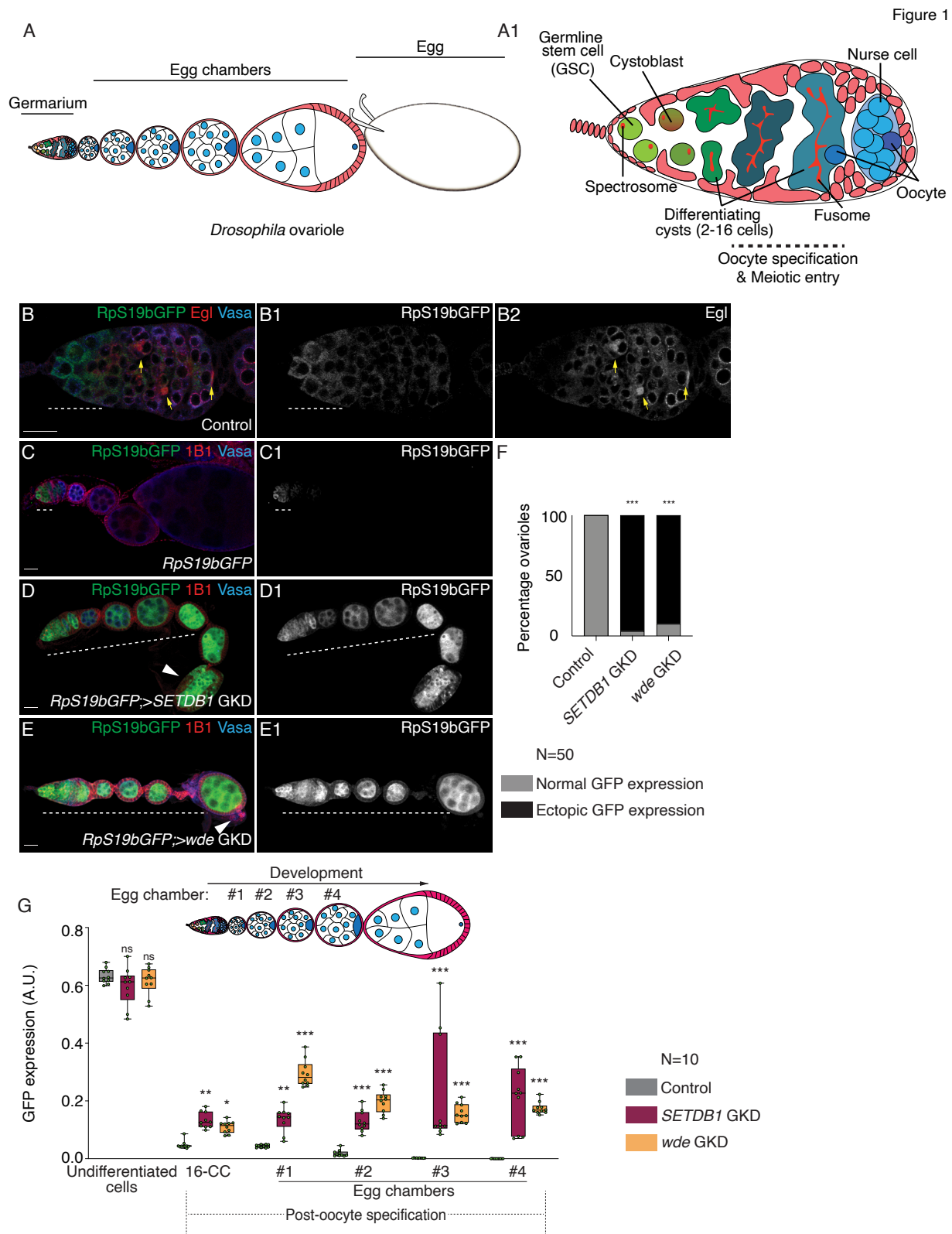602   was determined by Students t-test.

15

Figure1: *SETDB1* and *windei* are required for silencing *RpS19b* reporter during oogenesis

603
604
605

606

607 (A) A schematic of a *Drosophila* ovariole. The ovariole consists of germarium and egg chambers
608 corresponding to distinct developmental stages. Egg chambers are connected by somatic cells
609 (light red). During development, egg chambers grow and eventually give rise to a mature egg
610 (white).

611

612 (A1) A schematic of a *Drosophila* germarium, where germline stem cells (GSCs; light green) are
613 at close proximity to somatic niche (red). The GSC divides to give rise to daughter cells called
614 cystoblasts (dark green) which turns on a differentiation program. Both GSCs and cystoblasts are
615 marked by spectrosomes (red). Cystoblasts undergo four incomplete mitotic divisions, giving rise
616 to 2-, 4-, 8-, and 16-cell cysts (green), marked by fusomes (red). During the cyst stages germ
617 cells progress through meiotic cell cycle (prophase I). Upon 16-cell cyst formation, a single cell is
618 specified as the oocyte (dark blue) while the other 15 cells become nurse cells (light blue).

619

620 (B-B2) Confocal images of a germarium of a fly carrying *RpS19b-GFP* reporter transgene stained
621 for GFP (green, right grayscale), Egl (red, right grayscale) and Vasa (blue). GFP is expressed in
622 the single cells undifferentiated stages and early cyst stages (white dashed line), while Egl is
623 expressed in the differentiated cysts and localized to the specified oocyte (yellow arrows).

624

625 (C-E) Ovariole of control *RpS19b-GFP* (D-D1), GKD of *SETDB1* (E-E1) and *wde* (F-F1) stained
626 for GFP (green, right grayscale), Vasa (blue) and 1B1 (red). Depletion of these genes resulted in
627 characteristic phenotype of egg chambers not growing and mid oogenesis death (white solid
628 arrows). In addition, ectopic expression of *RpS19b*-GFP was observed in the egg chambers
629 (white dashed line).

630

631 (F) Quantification of ectopic RpS19b-GFP expression upon GKD of *SETDB1* or *wde* compared
632 to control ovaries (N= 50 ovarioles; 96% in *SETDB1* GKD and 90% in *wde* GKD compared to 0%
633 in control.) Statistical analysis was performed with Fisher's exact test on ectopic GFP expression;
634 *** = $p<0.001$.

635

636 (G) Arbitrary units (A.U.) quantification of RpS19b-GFP expression in the germarium and egg
637 chambers during development upon GKD of *SETDB1* (magenta) or *wde* (orange) compared to
638 control ovaries (black). GFP is expressed higher in single cells in the germarium, decreases in
639 the cyst stages, and then attenuated upon egg chamber formation. In *SETDB1* and *wde* GKD,
640 GFP expression persists in the egg chambers. Statistical analysis was performed with Dunnett's
641 multiple comparisons test; N= 10 ovarioles; ns = $p>0.05$, *=$p<0.05$, ** = $p<0.01$, *** = $p<0.001$.

642

643

644 Scale bars are 15 micron.

645

646

647

648

649
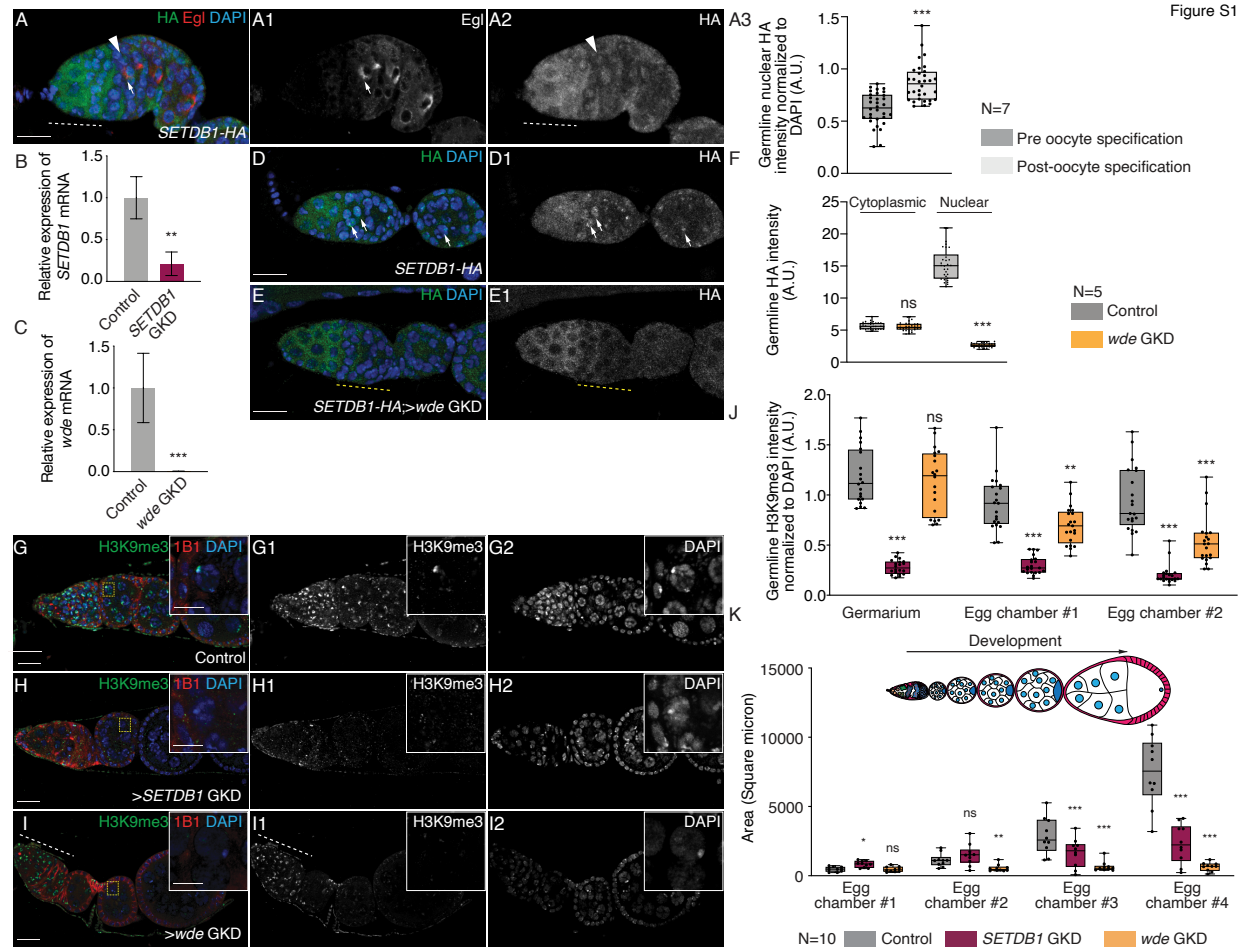
Supplementary Figure1: SETDB1/Wde mediated heterochromatin formation is required for silencing *RpS19b* reporter

(A-A3) Germarium of a fly carrying HA tagged SETDB1 stained for HA (green, right grayscale), oocyte marker Egl (red, right grayscale) and DAPI (blue). White arrows point at the specified oocyte. SETDB1 translocates from the cytoplasm (white dotted line) to the nucleus concurrent with oocyte specification (white solid arrow). Quantitation of HA level (A3) expressed as a ratio of nuclear SETDB1 to DAPI. Statistical analysis was performed with Welch's t-test; N= 7 germaria; ns = p>0.05, *=p<0.05, ** = p<0.01, *** = p<0.001

(B-C) qRT-PCR assaying the mRNA levels of *SETDB1* (B) and *wde* (C) in control and *SETDB1* and *wde* GKD respectively, normalized to control *rp49* mRNA levels and indicating knockdown of these genes (N=3, **=p<0.01, *** = p<0.001, Error bars are SEM, Student's t-test).

(D-F) SETDB1-HA ovariole (D-D1) and *SETDB1-HA* ovariole depleted of *wde* (E-E1) stained for HA (green, right grayscale) and Vasa (blue). Yellow arrows point at nuclear HA. GKD of *wde* shows that levels of HA in the nucleus is attenuated (yellow dotted line). (F) Quantification of germline HA levels in the cytoplasm in the undifferentiated stages and in the nucleus of the

18

670   differentiated stages in the germarium in ovaries depleted of *wde* (orange) compared to control

671   ovaries (gray). Statistical analysis was performed with Welch's t-test; N= 5 ovarioles; ns = $p > 0.05$,

672   *=$p < 0.05$, ** = $p < 0.01$, *** = $p < 0.001$.

673

674   (G-J) Ovariole of control *UAS-Dcr2;nosGAL4* (G-G1), GKD of *SETDB1* (H-H1) or *wde* (I-I1)

675   stained for H3K9me3 (green, right grayscale), DAPI (blue, right grayscale) and 1B1 (red). Nurse

676   cells from egg chamber highlighted by a dashed yellow square represent cells shown in the inset.

677   Control shows H3K9me3 is present throughout oogenesis in the germline. GKD of *SETDB1*

678   shows loss of H3K9me3 in all stages of the germline while depletion of *wde* results in decreased

679   H3K9me3 post-differentiation only in the egg chambers but not in germarium (white dotted line).

680   (J) Quantification of H3K9me3 expression in the germline normalized to DAPI level in ovaries

681   depleted of *SETDB1* (magenta) or *wde* (orange) compared to control ovaries (gray). Statistical

682   analysis was performed with Dunnett's multiple comparisons test; N= 10 ovarioles; ns = $p > 0.05$,

683   *=$p < 0.05$, ** = $p < 0.01$, *** = $p < 0.001$.

684

685   (K) Quantification of area of germarium and egg chambers during development in *SETDB1*

686   (magenta) or *wde* (orange) GKD ovaries compared to control ovaries (gray). Statistical analysis

687   was performed with Dunnett's multiple comparisons test; N= 10 ovarioles; ns = $p > 0.05$, *=$p < 0.05$,

688   ** = $p < 0.01$, *** = $p < 0.001$.

689

690   Scale bars are 15 micron and for main images and scale bar for insets is 4 micron.
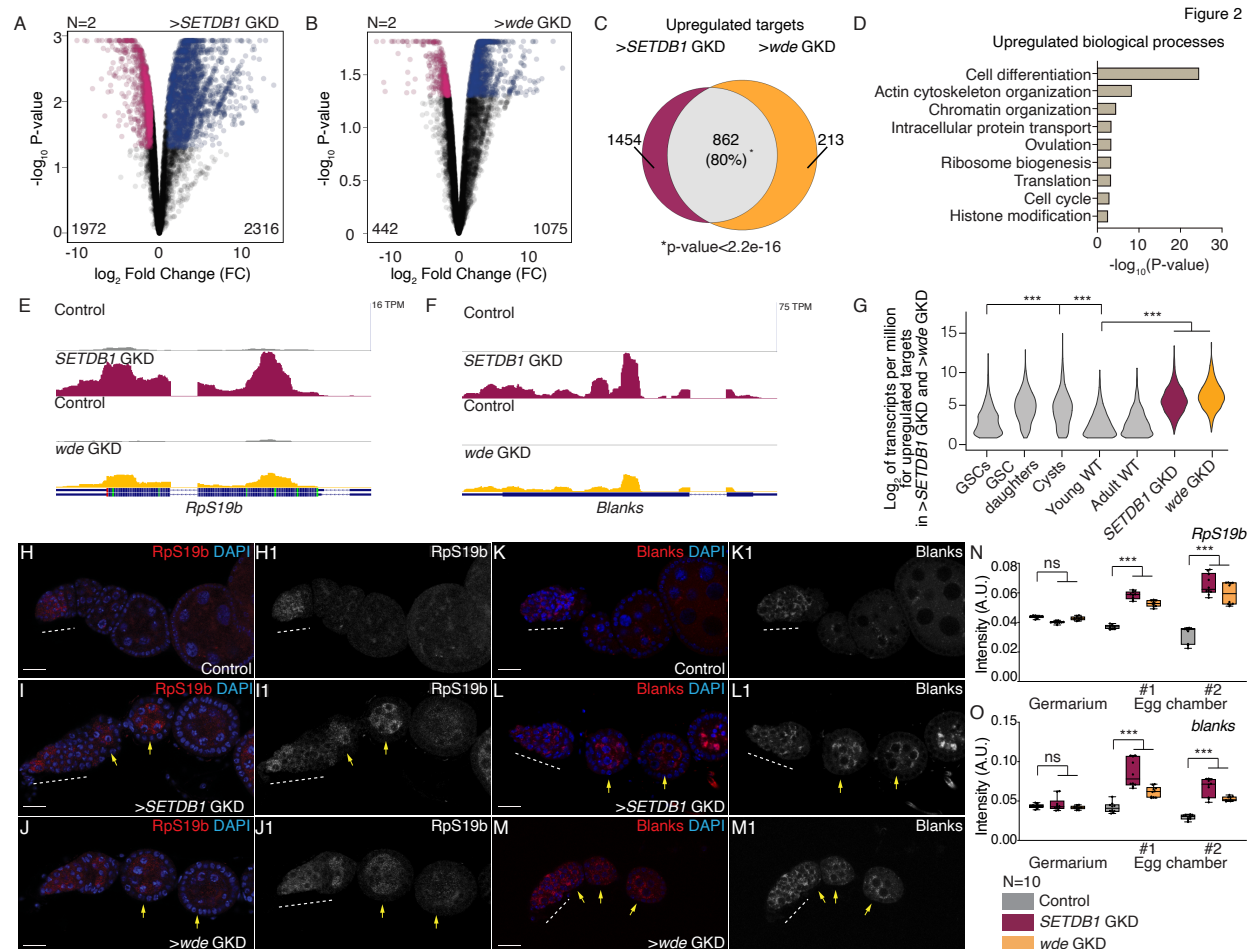
691

692

693

19

Figure 2: SETDB1/Wde represses a cohort of early oogenesis genes

(A-B) Volcano plots of $-\text{Log}_{10}$P-value vs. Log_2Fold Change (FC) of (A) *SETDB1* and (B) *wde* GKD ovaries compared to control *UAS-Dcr2;NG4NGT* flies. Pink dots represent significantly downregulated transcripts and blue dots represent significantly upregulated transcripts in *SETDB1*, and *wde* GKD ovaries compared with control ovaries (FDR = False Discovery Rate < 0.05 and genes with 1.5-fold or higher change were considered significant).

(C) Venn diagram of upregulated genes from RNA-seq of *SETDB1* and *wde* GKD ovaries compared to *UAS-Dcr2;NG4NGT*. 862 targets are shared between GKD of *SETDB1* and *wde*, suggesting that SETDB1 and Wde co-regulate a specific cohort of genes.

(D) The most significant biological process GO terms of shared upregulated genes in ovaries depleted of *SETDB1* and *wde* compared to *UAS-Dcr2;NG4NGT* control (FDR from p-values using a Fisher's exact test), showing differentiation as one of the significant processes regulated by SETDB1/Wde.

20

713 (E-F) RNA-seq track showing that *RpS19b* and *blanks* is upregulated upon GKD of *SETDB1* and
714 *wde*.

715

716 (G) Violin plot of mRNA levels of the 862 shared upregulated targets in ovaries enriched for GSCs,
717 cystoblasts, cysts, and whole ovaries, showing that the shared targets between *SETDB1* and *wde*
718 are most highly expressed up to the cyst stages, that then tapers off in whole ovaries. Statistical
719 analysis performed with Hypergeometric test; *** indicates $p < 0.001$.

720

721 (H-J1) Confocal images of germaria probed for *RpS19b* mRNA (red, grayscale) and DAPI (blue)
722 in *UAS-Dcr2;NG4NGT* (H-H1) showing *RpS19b* RNA expression restricted to early stages of
723 oogenesis and in GKD of *SETDB1* (I-I1) and *wde* (J-J1) ovarioles showing *RpS19b* mRNA
724 expression is expanded to egg chambers.

725

726 (K-M1) Confocal images of germaria probed for *blanks* mRNA (red, grayscale) and DAPI (blue)
727 in *UAS-Dcr2;NG4NGT* (K-K1) showing *blanks* mRNA expression restricted to early stages of
728 oogenesis and in GKD of *SETDB1* (L-L1) and *wde* (M-M1) ovarioles where *blanks* mRNA
729 expression is expanded to egg chambers.

730

731 (N-O) Quantification of fluorescence intensity of *RpS19b* (N) and *blanks* (O) mRNAs in the
732 germarium and egg chambers during development in ovaries depleted of *SETDB1* (magenta) or
733 *wde* (orange) compared to control ovaries (gray). Statistical analysis was performed with
734 Dunnett's multiple comparisons test; N= 10 ovarioles; ns = $p > 0.05$, *=$p < 0.05$, ** = $p < 0.01$, *** =
735 $p < 0.001$.

736
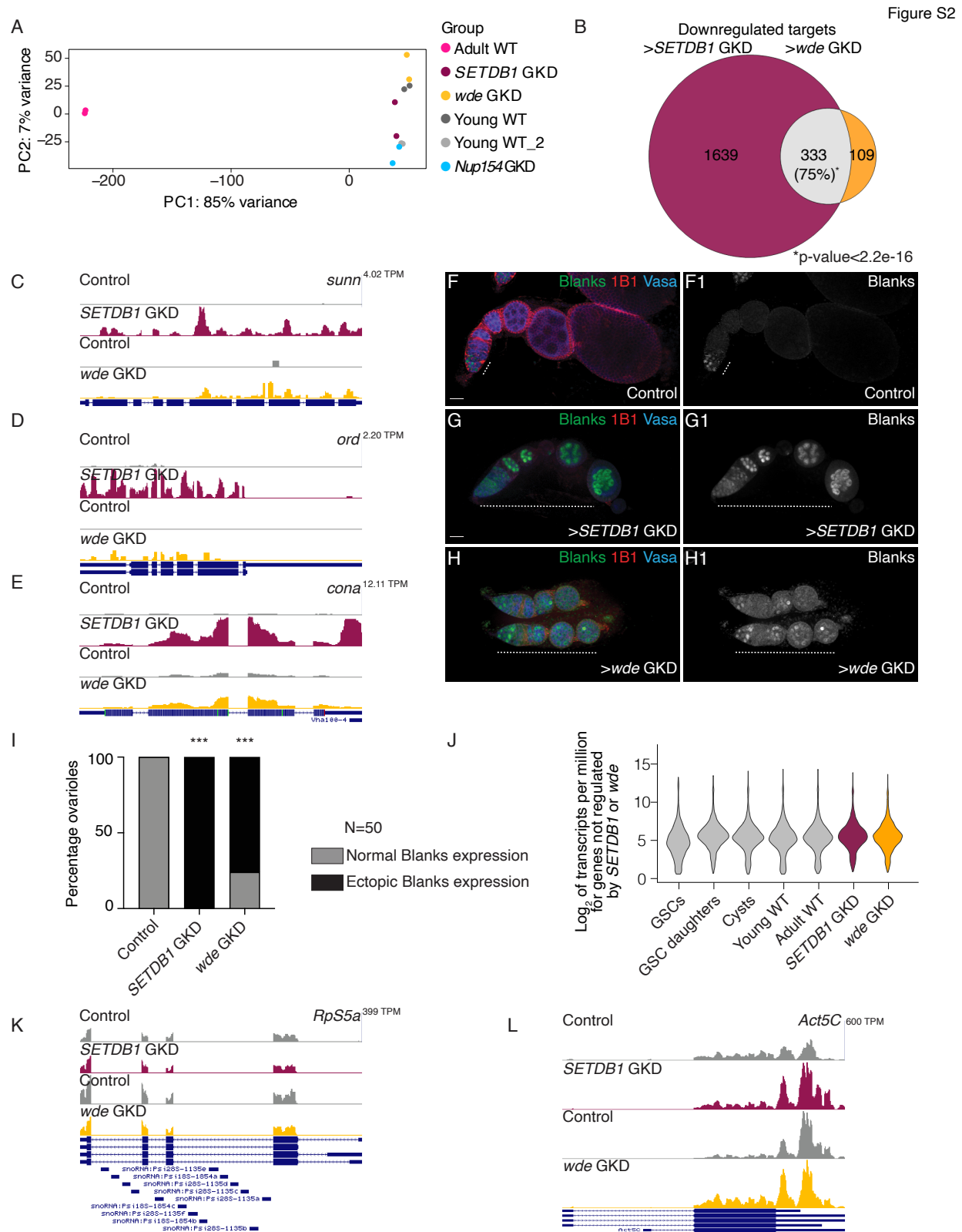
Figure S2

Supplementary Figure 2: SETDB1/Wde represses a cohort of genes that are broadly expressed prior to oocyte specification

(A) Principal Component Analysis (PCA) comparing RNA-seq data sets including adult WT, young WT, *SETDB1* GKD and *wde* GKD indicates that the *SETDB1, wde* and *Nup154* GKD samples are similar to young WT.

(B) Venn diagram of downregulated genes from RNA-seq of *SETDB1* and *wde* GKD ovaries compared to *UAS-Dcr2;NG4NGT*. 333 targets are shared between *SETDB1* and *wde* GKD.

(C-E) RNA-seq track showing that synaptonemal complex members *sunn, ord* and *cona* are upregulated upon *SETDB1* and *wde* GKD*.*

(F-H1) Confocal images of *UAS-Dcr2;NG4NGT* (C-C1), *SETDB1* (D-D1) and *wde* (E-E1) GKD ovarioles stained for 1B1 (red), Vasa (blue) and Blanks protein (green and grayscale) showing expanded Blanks expression in both *SETDB1* and *wde* GKD egg chambers (arrow).

(I) Quantification of percentage ovarioles with ectopic *Blanks* expression (black) in *SETDB1* or *wde* GKD ovaries to control ovaries (N= 50 ovarioles; 100% in *SETDB1* GKD and 82% in *wde* GKD compared to 0% in control.) Statistical analysis was performed with Fisher's exact test on ectopic *Blanks* expression; *** = p<0.001.

(J) Violin plot of mRNA levels of the genes not regulated by *SETDB1* or *Wde* in ovaries enriched for GSCs, cystoblasts, cysts, and whole ovaries, showing that *SETDB1* and *wde* non-targets are not attenuated in the later egg chamber ovaries compared to earlier stages of oogenesis.

(K-L) RNA-seq track showing that levels of non-targets *RpS5a* and *Act5C* are not affected by *SETDB1* or *wde* GKD.
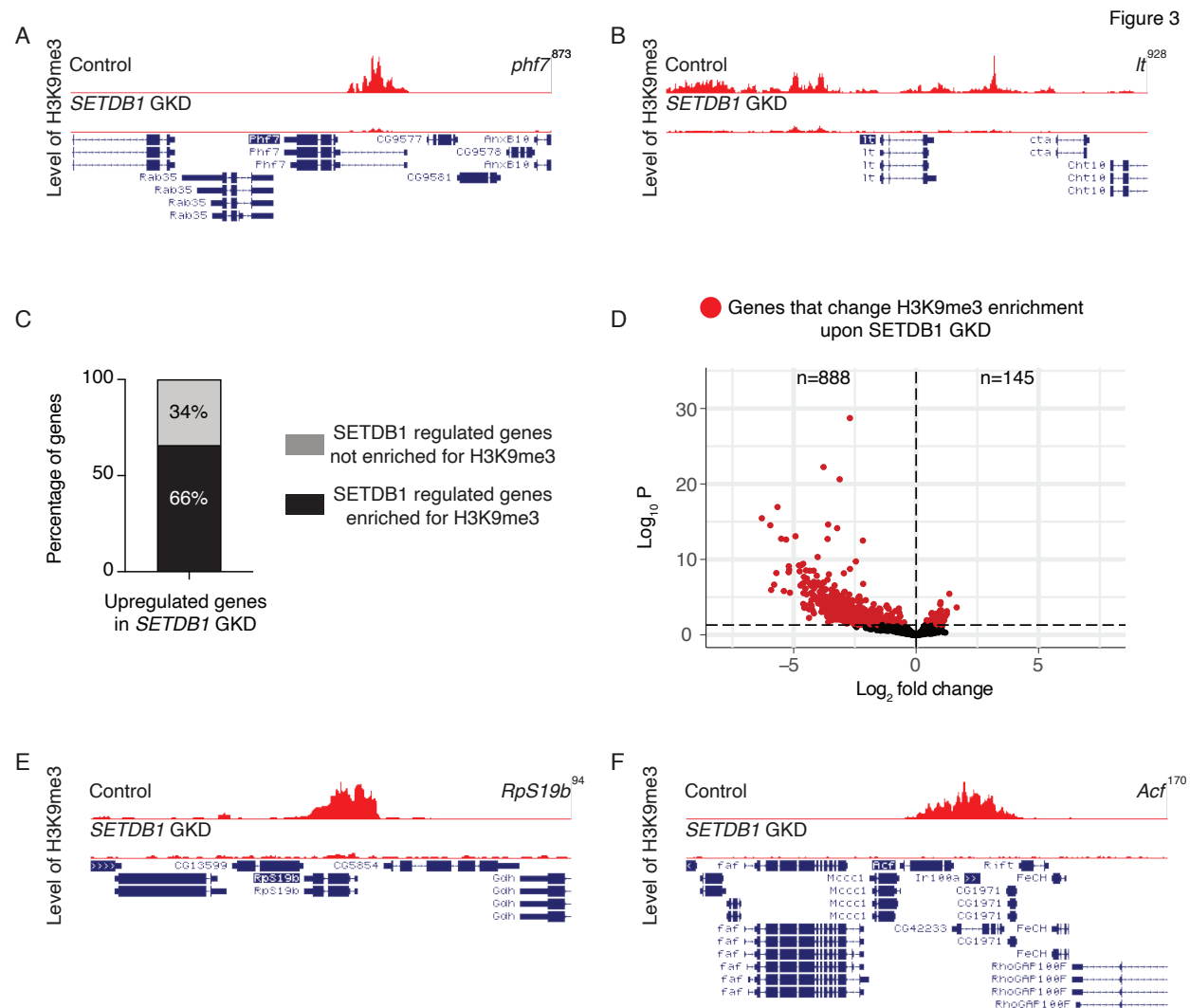
23

Figure 3: SETDB1 promotes silencing of early oogenesis genes by regulating levels of H3K9me3

(A-B) Tracks showing level of H3K9me3 on previously validated and known heterochromatic genes *phf7* and *lt* respectively.

(C) Bar graph showing genes regulated by *SETDB1* that are enriched for H3K9me3 on the gene body. 1593 (black) out of 2316 (gray) genes upregulated upon loss of *SETDB1* are enriched for H3K9me3.

(D) Volcano plot showing changes in H3K9me3 in *SETDB1* GKD compared to WT. Genes that lose H3K9me3 are shown on the left (red). 888 genes lose H3K9me3 after *SETDB1* GKD.

(E-F) Tracks showing level of H3K9me3 on target genes. Our data shows loss of H3K9me3 on SETDB1 targets *RpS19b* and *Acf* respectively (E-F) suggesting they are directly regulated by SETDB1.

787
788

Figure S3

789
790
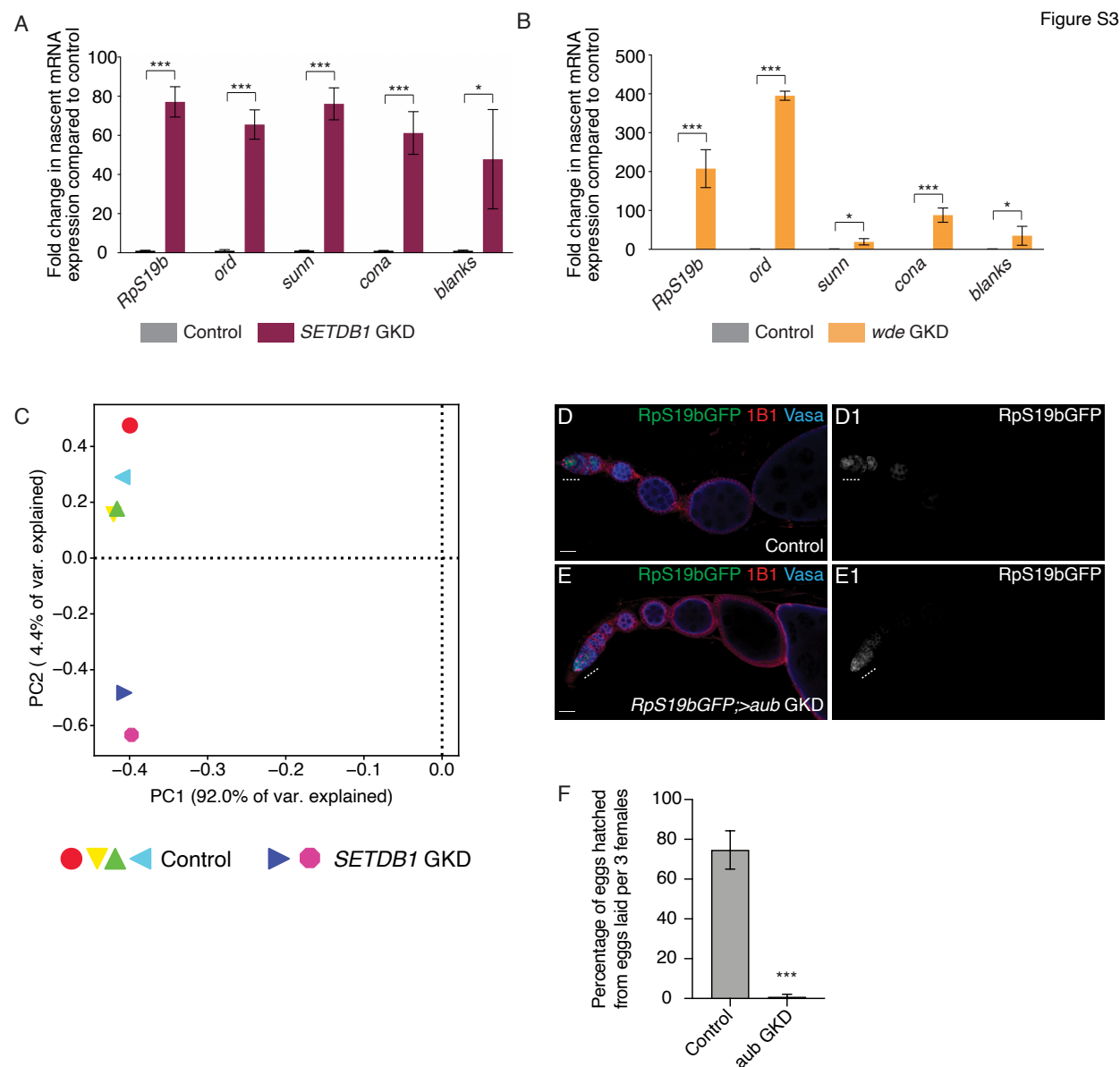
791 **Supplementary Figure 3: SETDB1/Wde transcriptionally silences expression of a subset of**
792 **early oogenesis genes**

793

794 (A) qRT-PCR assaying the pre-mRNA levels of *SETDB1*-regulated target genes, including
795 *RpS19b*, *ord*, *sunn*, *cona* and *blanks* in control and GKD of *SETDB1* shows that these genes are
796 upregulated (n=3, *** indicates p<0.001, Error bars are SEM, Student's t-Test).

797

798 (B) qRT-PCR assaying the pre-mRNA levels of *Wde*-regulated target genes, including *RpS19b*,
799 *ord*, *sunn*, *cona* and *blanks* in control and GKD of *Wde* shows that pre-mRNA levels of these

25

800   genes are upregulated (n=3, * = $p \leq 0.05$, ** = $p<0.01$, *** = $p<0.001$, Error bars are SEM,
801   Student's t-Test).
802
803   (C) Principal Component Analysis (PCA) comparing CUT&RUN data sets for control and *SETDB1*
804   GKD.
805
806   (D-E1) Ovariole from control *RpS19b*-GFP (D-D1) and GKD of *aub* (E-E1) stained for GFP (green,
807   right grayscale), Vasa (blue) and 1B1 (red). Depletion of this gene shows normal development of
808   the egg chambers and there was no ectopic expression of *RpS19b*-GFP in the egg chambers
809   suggesting SETDB1-mediated silencing of *RpS19b-GFP* is independent of piRNA pathway.
810
811   (F) Fertility assay of *aub* GKD indicating there was significant decrease in number of adult flies
812   that eclosed from the eggs laid by *aub* GKD flies compared to those from control flies (n=3 trials).
813   *** = $p < 0.001$, Tukey's post-hoc test after one-way ANOVA.
814

Figure 4

815
816

27
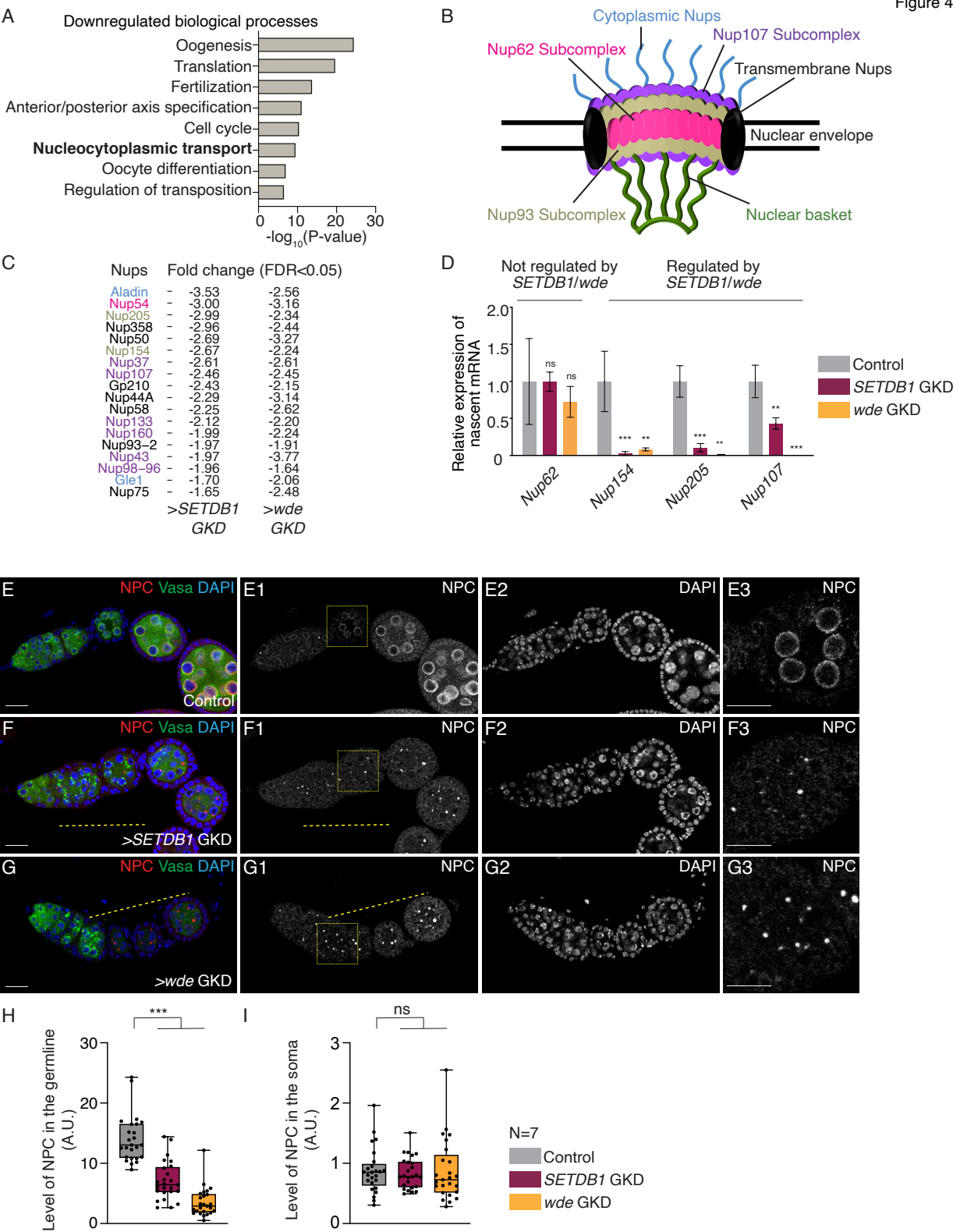
817 **Figure 4: SETDB1/Wde promotes expression of a subset of nucleoporin genes and NPC**
818 **formation**
819
820 (A) The significant biological process GO terms of common downregulated genes in *SETDB1* or
821 *wde* GKD ovaries compared to *UAS-Dcr2;NG4NGT* control (FDR from p-values using a Fisher's
822 exact test), showing nucleocytoplasmic transport as one of the significant processes regulated by
823 SETDB1/Wde.
824
825 (B) A schematic of the Nucleopore Complex (NPC) showing cytoplasmic ring, nuclear ring and
826 basket facing nucleoplasm and a central scaffold spanning the nuclear membrane. NPC is
827 composed of several subcomplexes and ~30 nucleoporins (nups).
828
829 (C) Table showing levels of 18 nucleoporin mRNAs that are down regulated 1.5 or more fold in
830 both *SETDB1* or *wde* GKD ovaries compared to *UAS-Dcr2;NG4NGT* control ovaries.
831
832 (D) qRT-PCR assaying the pre-mRNA levels of *SETDB1* and *Wde*-regulated *Nup* genes,
833 including *Nup154*, *Nup205* and *Nup107* are decreased compared to control *UAS-Dcr2;NG4NGT*
834 while levels of non-target *Nup62* pre-mRNA is not affected (control level vs *SETDB1* GKD and
835 *wde* RNA in=3, ** = p<0.01, *** = p<0.001, Error bars are SEM, Student's t-Test).
836
837 (E-G3) Ovariole and egg chamber images of control *UAS-Dcr2;NG4NGT* (E-E3), GKD of *SETDB1*
838 (F-F3) and *wde* (G-G3) stained for NPC (red, grayscale), Vasa (green) and DAPI (blue). NPC
839 staining was done using mab414 antibody. Depletion of *SETDB1* shows reduced expression of
840 NPC in the egg chambers suggesting SETDB1 regulates expression of several nucleoporins
841 which in turn regulates formation of NPC.
842
843 (H-I) A.U. quantification of NPC level in the germline (H) and soma (I) in *SETDB1* and *wde* GKD
844 ovaries compared to *UAS-Dcr2;NG4NGT* control. Statistical analysis was performed with
845 Dunnett's multiple comparisons test; N= 25 ovariole for germline and 15 for somatic quantitation;
846 ns = p>0.05, * = p ≤ 0.05, ** = p<0.01, *** = p<0.001.
847
848
849

28

Figure S4

850
851
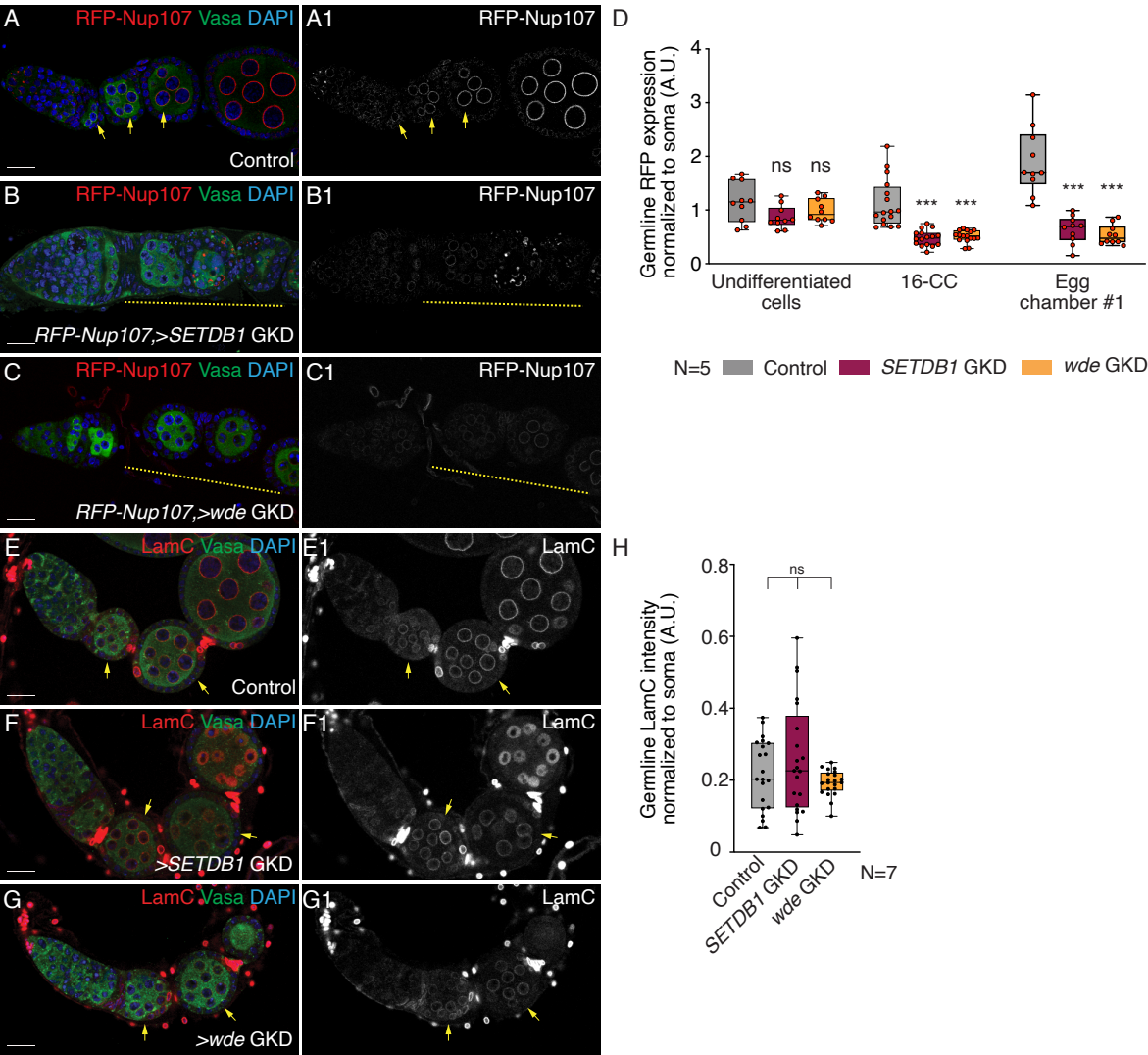
852 **Supplementary Figure 4: SETDB1/Wde promotes NPC formation without affecting Lamin**
853 **C**
854
855 (A-C1) Ovariole of control *RFP-Nup107* A-A1), GKD of *SETDB1* (B-B1) and *wde* (C-C1) stained
856 for RFP (red, right grayscale), Vasa (green) and DAPI (blue). Depletion of *SETDB1* or *wde* shows
857 lower expression of RFP in the egg chambers (yellow line) suggesting *SETDB1/wde* regulates
858 expression of Nup107.
859
860 (D) A.U. quantification of RFP level in the germline normalized to soma in *SETDB1-* and *wde-*
861 GKD ovaries compared to control. Statistical analysis was performed with Dunnett's multiple
862 comparisons test; N= 5 ovariole; ns = p>0.05, * = p ≤ 0.05, ** = p<0.01, *** = p<0.001.
863
864 (E-G1) Ovariole of control *UAS-Dcr2;NG4NGT* (E-E2), GKD of *SETDB1* (F-F2) and *wde* (G-G2)
865 stained for LamC (red, right grayscale), Vasa (green) and DAPI (blue). Depletion of *SETDB1* or
866 *wde* shows similar expression of LamC in the egg chambers suggesting *SETDB1* or *wde*
867 depletion does not affect expression of LamC.
868
869 (H) A.U. quantification of LamC level in the germline normalized to soma in *SETDB1-* and *wde-*
870 GKD ovaries compared to *UAS-Dcr2;NG4NGT* control. Statistical analysis was performed with
871 Dunnett's multiple comparisons test; N= 7 ovariole; ns = p>0.05.
872
873
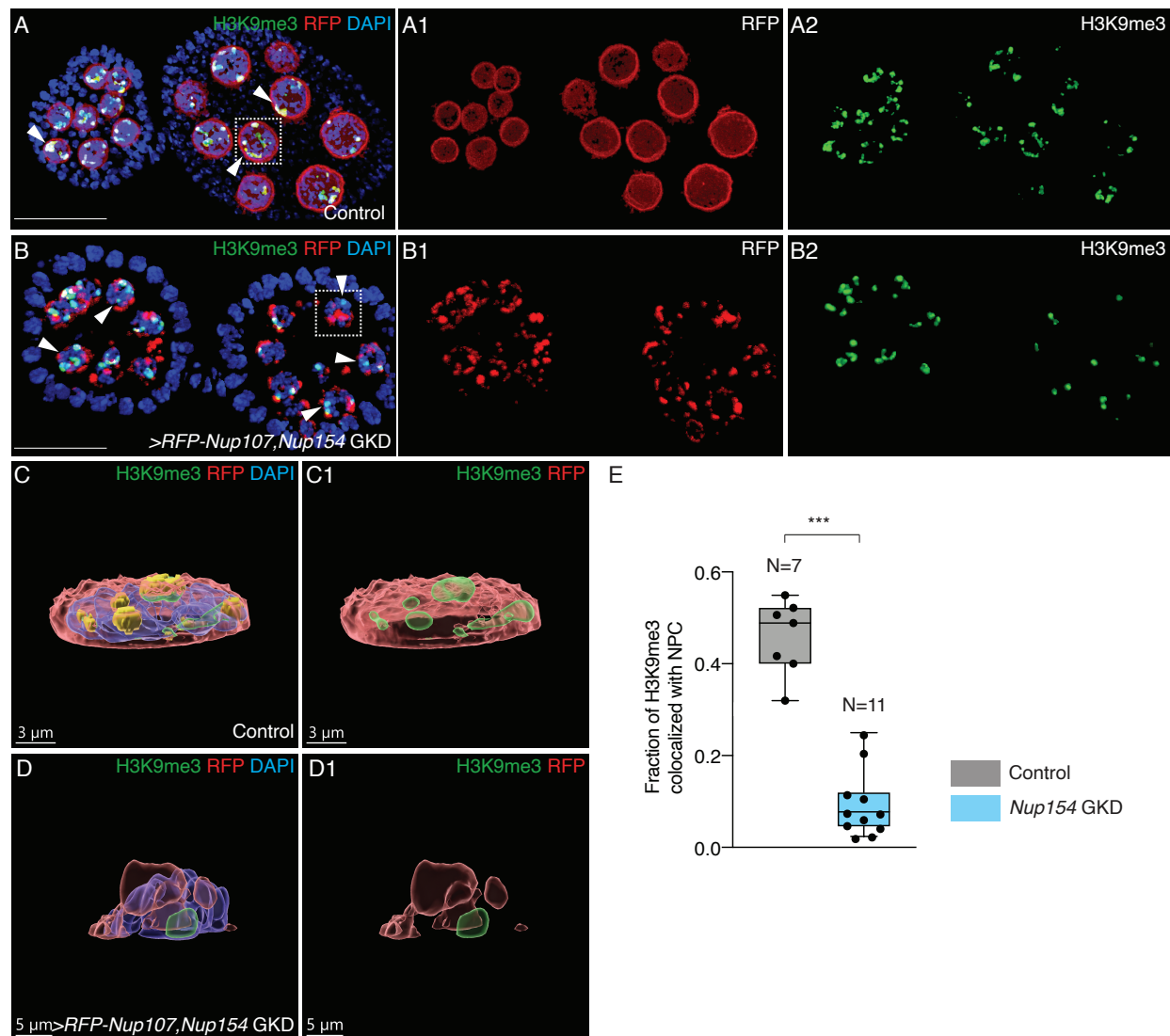874
875
876
877
878

Figure 5

879
880
881 **Figure 5: H3K9me3 heterochromatin colocalizes with NPC component Nup107 at the**
882 **nuclear periphery**
883
884 (A-A2) Egg chambers of control *UAS-Dcr2;NG4NGT* ovariole showing RFP-Nup107 (red, right
885 red channel), H3K9me3 (green, right green channel). Heterochromatin is seen in close
886 association with NPC (white arrows). Colocalized fraction is shown in yellow.
887
888 (B-B2) Egg chambers of *Nup154* GKD ovariole showing significant decrease in the colocalization
889 (white arrows) between RFP-Nup107 (red, right red channel) and H3K9me3 (green, right green
890 channel).
891
892 (C-C1) 3D reconstruction of a single nuclei (white dotted box in A) from an egg chamber of control
893 *UAS-Dcr2;NG4NGT* ovariole. Yellow channel shows colocalized fraction of RFP-Nup107 (red)

894   and H3K9me3 (green). This shows that H3K9me3 heterochromatin domains (green) are formed
895   at the nuclear periphery and closely associate with Nup107.
896

897   (D-D1) 3D reconstruction of a single nuclei (white dotted box in B) from an egg chamber of
898   *Nup154* GKD showing colocalization (yellow) of H3K9me3 with Nup107. This shows significant
899   reduction in colocalized fraction of H3K9me3 with Nup107.
900

901   (E) Quantification of levels of H3K9me3 that colocalizes with NPC in the germline of control
902   ovarioles (gray) in contrast to *Nup154* GKD ovarioles (blue). Quantitative object based
903   colocalization was measured in Imaris software, *** = $p<0.001$, one-tailed Students t-Test.
904
905
906
907
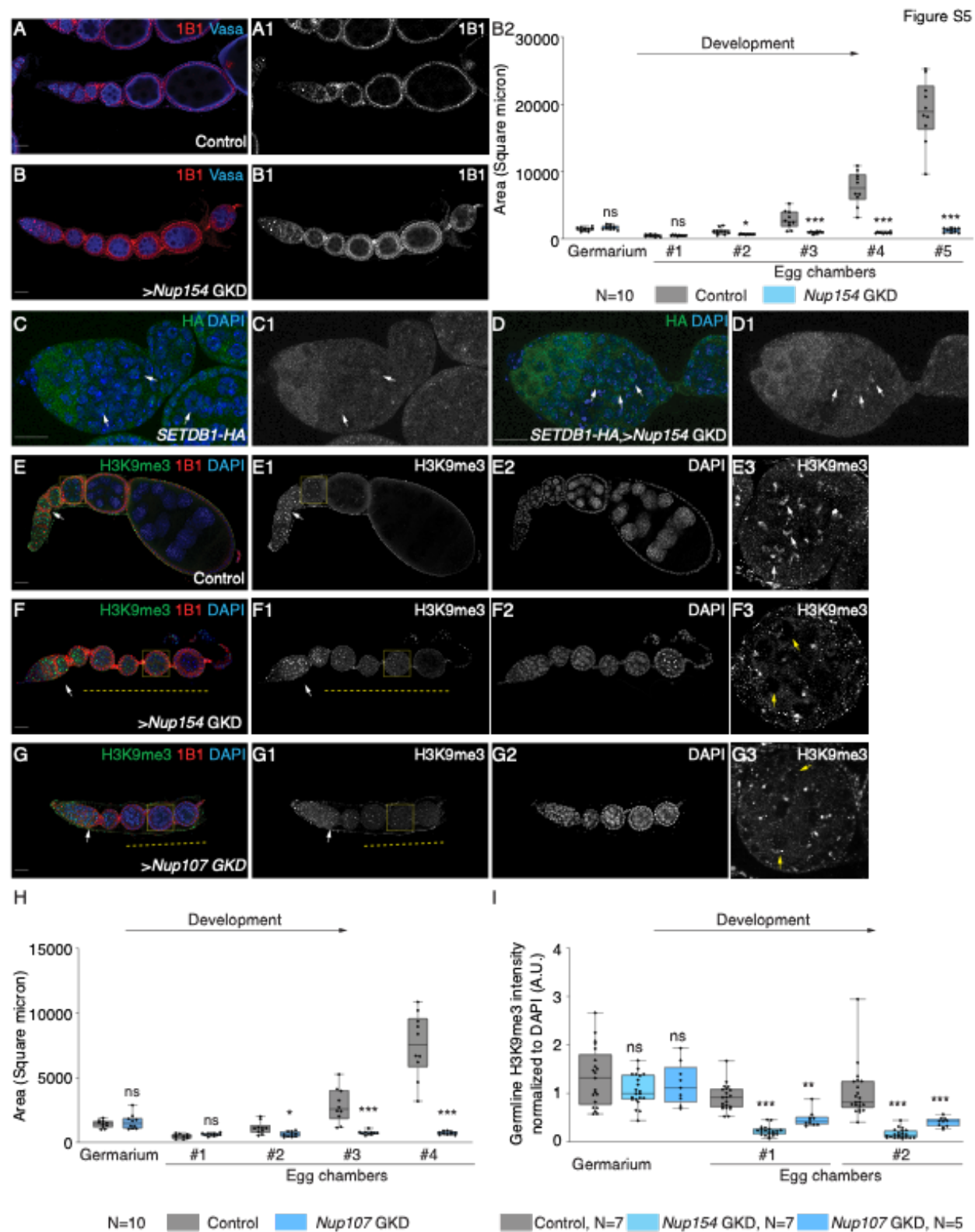
Supplementary Figure 5: NPC is required for maintaining heterochromatin

911   (A-B2) Ovariole of control *UAS-Dcr2;NG4NGT* (A-A1) and GKD of *Nup154* (B-B1) stained for 1B1
912   (red, right grayscale) and Vasa (blue). Control shows normal development of egg chambers while
913   *Nup154* GKD shows egg chambers that do not grow. (B2) Quantification of area of germarium
914   and egg chambers during development in ovaries depleted of *Nup154* (blue) compared to control
915   ovaries (gray). Statistical analysis was performed with Student's t-test; N= 10 ovarioles; ns =
916   p>0.05, * = p ≤ 0.05, ** = p<0.01, *** = p<0.001.

918   (C-D) Germaria of flies carrying HA tagged SETDB1 (C-C1) and GKD of *Nup154* (D-D1) stained
919   for HA (green, right grayscale) and Vasa (blue). White arrows point at nuclear HA. Depletion of
920   germline *Nup154* shows HA is present in the nucleus.

922   (E-G3) Ovariole and egg chamber of control *UAS-Dcr2;NG4NGT* (E-E3), GKD of *Nup154* (F-F3)
923   and *Nup107* (G-G3) stained for H3K9me3 (green, right grayscale), DAPI (blue, right grayscale)
924   and 1B1 (red). Control shows H3K9me3 expression throughout oogenesis in the germline.
925   Depletion *Nup154* and *Nup107* results in decreased H3K9me3 (yellow dotted line) after
926   differentiation in the egg chambers. Late-stage egg chamber (yellow dotted squares) images
927   show decreased or loss of H3K9me3 in *Nup154* and *Nup107* GKD nurse cells (yellow arrows).

929   (H) Quantification of area of germarium and egg chambers during development in ovaries
930   depleted of *Nup107* (blue) compared to control ovaries (gray). Statistical analysis was performed
931   with Student's t-test; N= 10 ovarioles; ns = p>0.05, * = p ≤ 0.05, ** = p<0.01, *** = p<0.001.

933   (I) Quantification of H3K9me3 levels in the germline normalized to DAPI level in ovaries depleted
934   of *Nup154* (blue) and *Nup107* (blue) compared to control ovaries (gray). Statistical analysis was
935   performed with Dunnett's multiple comparisons test; ns = p>0.05, *=p<0.05, ** = p<0.01, *** =
936   p<0.001.

Figure 6

940
941

35
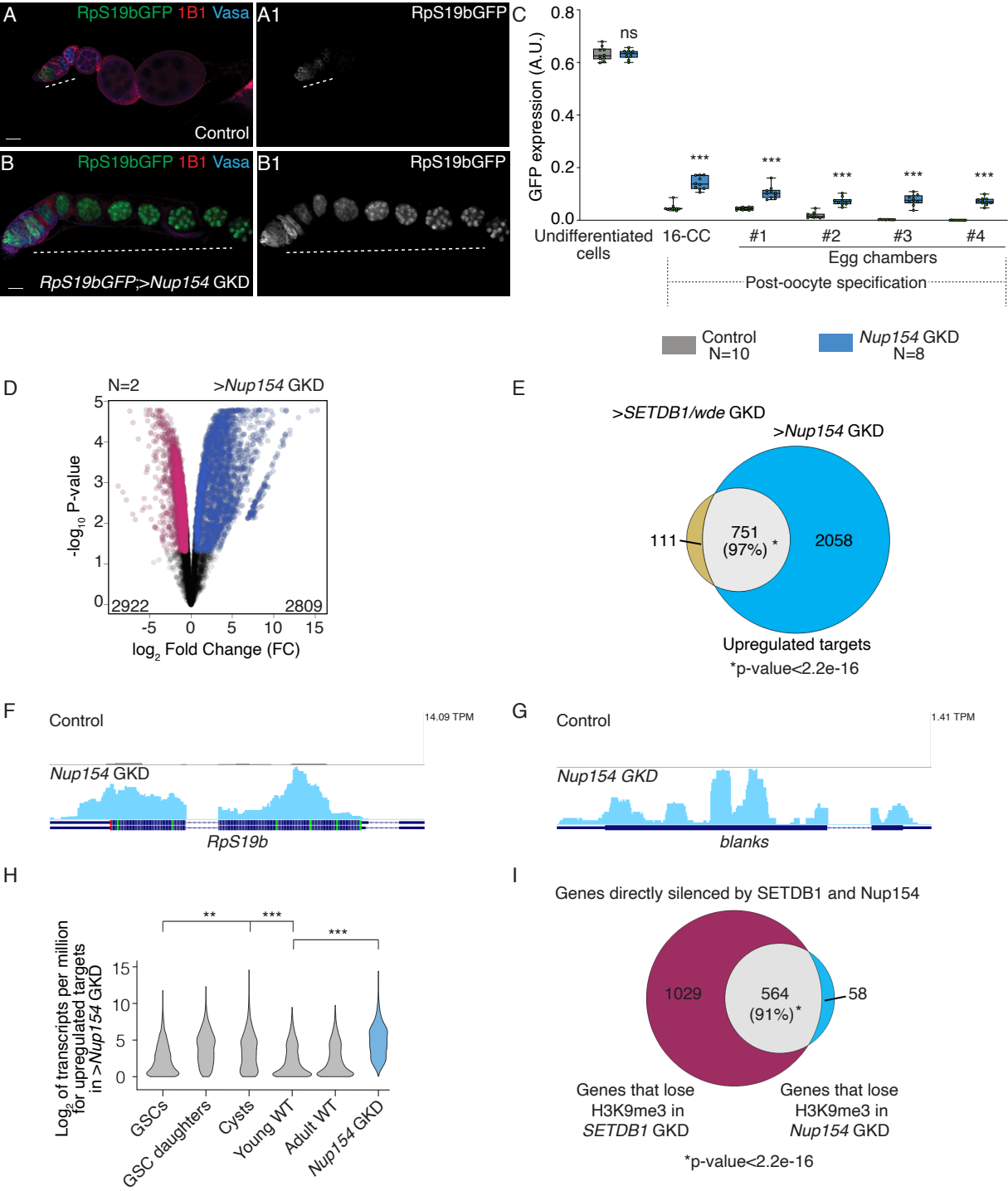
Figure 6: Nup154 is required for silencing a cohort of genes expressed during early oogenesis

(A-B1) Ovariole of control *RpS19b-GFP* (A-A1), GKD of *Nup154* (B-B1) stained for GFP (green, right grayscale), Vasa (blue) and 1B1 (red). Depletion of *Nup154* shows characteristic phenotype where the egg chambers did not grow and there was ectopic expression of *RpS19b*-GFP in the egg chambers (white dashed line).

(C) Arbitrary units (A.U.) quantification of RpS19b-GFP expression in the germarium and egg chambers during development upon GKD of *Nup154* (blue) compared to control ovaries (gray). GFP is expressed higher in single cells in the germarium, decreases in the cyst stages, and then attenuated upon egg chamber formation in control. In *Nup154* GKD, GFP expression persists in the egg chambers. Statistical analysis was performed with Dunnett's multiple comparisons test; N= 10 and 8 ovarioles for control and *Nup154* GKD respectively; ns = $p>0.05$, *=$p<0.05$, ** = $p<0.01$, *** = $p<0.001$.
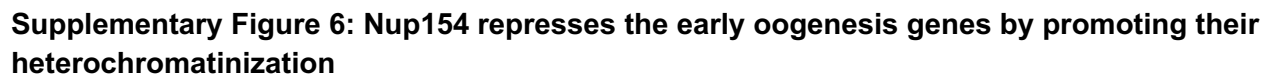
(D) Volcano plots of $-\text{Log}_{10}$P-value vs. Log_2Fold Change (FC) of mRNAs that show changes in *Nup154* GKD compared to *UAS-Dcr2;NG4NGT* control ovaries. Pink dots represent significantly downregulated transcripts and blue dots represent significantly upregulated transcripts in *Nup154* GKD ovaries compared with control ovaries (FDR = False Discovery Rate < 0.05 and 1.5-fold or higher change were considered significant).

(E) Venn diagram of upregulated overlapping genes from RNA-seq of *SETDB1* and *wde* and genes from *Nup154* germline depleted ovaries compared to *UAS-Dcr2;NG4NGT*. 751 upregulated targets are shared between *SETDB1, wde* and *Nup154* GKD, suggesting that *Nup154* and *SETDB1* function in co-regulating a specific set of genes.

(F-G) RNA-seq track showing that *RpS19b* (F) and *blanks* (G) are upregulated upon germline depletion of *Nup154*.

(H) Violin plot of mRNA levels of the 2809 upregulated targets in ovaries enriched for GSCs, cystoblasts, cysts, and whole ovaries, showing that the upregulated targets of *Nup154* are most highly enriched upto the cyst stages, and then tapers off in whole ovaries. Statistical analysis performed with Hypergeometric test; *** indicates $p<0.001$.

(I) Venn diagram showing overlapping genes that lose H3K9me3 after depletion of both *SETDB1* and *Nup154* in the germline. 622 genes lose H3K9me3 after *Nup154* GKD out of which 564 genes are also directly silenced by SETDB1, suggesting co-regulation of these genes by both SETDB1 and Nup154.

36

985
986
987 **Supplementary Figure 6: Nup154 represses the early oogenesis genes by promoting their**
988 **heterochromatinization**

989

990   (A-C1) Ovariole from control *RpS19b*-GFP (A-A1), GKD of *Nup107* (B-B1) and *Nup62* (C-C1)
991   stained for GFP (green, right grayscale), Vasa (blue) and 1B1 (red). Depletion of these *Nups*
992   shows characteristic phenotype where the egg chambers do not grow and there is ectopic
993   expression of *RpS19b*-GFP in the egg chambers (white dashed line).

994

995   (D) A.U. quantification of ectopic RpS19b-GFP expression in the germarium and egg chambers
996   with development in ovaries of *Nup107* (teal) and *Nup62* (light blue) GKD compared to control
997   ovaries (gray). Statistical analysis was performed with Dunnett's multiple comparisons test; ns =
998   p>0.05, ** = p<0.01, *** = p<0.001.

999

1000 (E) Venn diagram of down regulated overlapping genes from RNA-seq of *SETDB1* and *wde*
1001 regulated genes with *Nup154* GKD ovaries compared to *UAS-Dcr2;NG4NGT*. 299 down
1002 regulated targets are shared between *SETDB1, wde* and *Nup154* GKD, suggesting that Nup154
1003 and SETDB1 function in co-regulating a specific set of genes.

1004

1005 (F-H) RNA-seq track showing that synaptonemal complex members *sunn, ord* and *cona* are
1006 upregulated upon germline depletion of *Nup154.*

1007

1008 (I) Violin plot of mRNA levels of the genes not regulated by *Nup154* in ovaries enriched for GSCs,
1009 cystoblasts, cysts, and young and adult whole ovaries, showing that the non-targets of *Nup154*
1010 are not silenced in the ovaries compared to cyst stages and whole ovaries. Statistical analysis
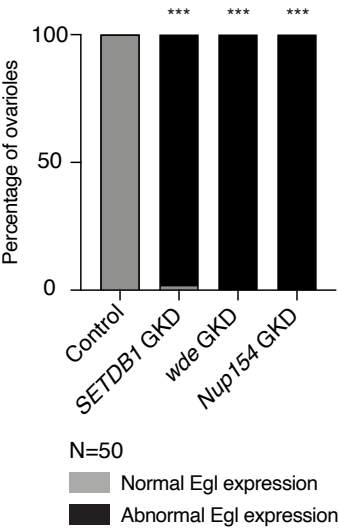1011 performed with Hypergeometric test; *** indicates p<0.001.

1012

1013 (J) RNA-seq track showing that upon germline depletion of *Nup154, Act5C* is unaffected.

1014

1015 (K-L) Tracks showing level of H3K9me3 on target genes. H3K9me3 is depleted on *Nup154* targets
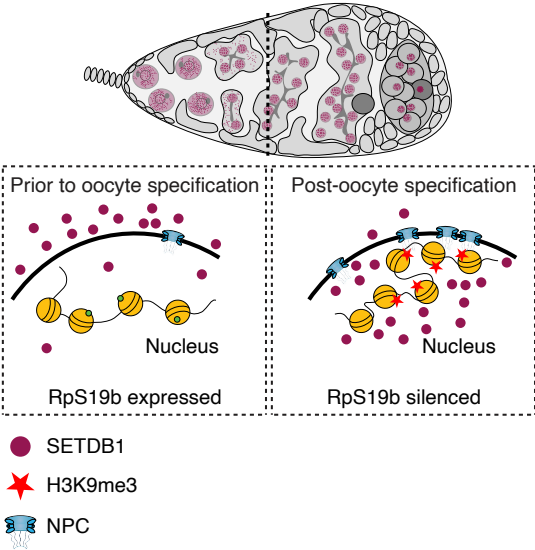1016 *RpS19b* and *Acf* respectively.

1017
1018
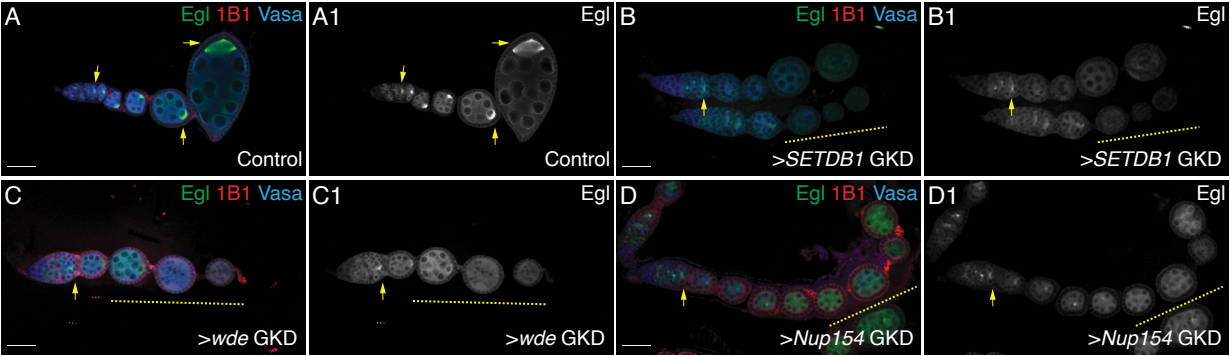
Figure 7

1019
1020
1021

1022 **Figure 7: Silencing of early oogenesis genes mediated by SETDB1, Wde and Nup154 is**
1023 **required for maintenance of oocyte fate**
1024
1025 (A-D1) Ovarioles of control *UAS-Dcr2;NG4NGT* (A-A1), GKD of *SETDB1* (B-B1), *wde* (C-C1) and
1026 *Nup154* (D-D2) stained for Egl (green, right grayscale), Vasa (blue) and 1B1 (red). Control shows
1027 proper oocyte specification with one oocyte in each egg chamber. Depletion of *SETDB1*, *wde* and
1028 *Nup154* in the germline results in initial oocyte specification (yellow arrow) which is then lost in
1029 the subsequent egg chambers (yellow dashed line).
1030
1031 (E) Quantification of percentage ovarioles with abnormal/loss of Egl expression (black) in ovaries
1032 depleted of *SETDB1* or *wde* or *Nup154* compared to control ovaries (gray) (N= 50 ovarioles; 98%
1033 in *SETDB1* GKD and 100% in *wde* and *Nup154* GKD compared to 0% in control.) Statistical
1034 analysis was performed with Fisher's exact *** = p<0.001.
1035
1036 (F) A model showing that nuclear translocation of SETDB1 after differentiation promotes
1037 heterochromatin formation mediated by deposition of H3K9me3 mark. This heterochromatin
1038 promotes increased NPC formation which then helps maintain heterochromatin.
1039
1040

40

References

Ables, E.T., 2015. Drosophila Oocytes as a Model for Understanding Meiosis: An Educational Primer to Accompany "Corolla Is a Novel Protein That Contributes to the Architecture of the Synaptonemal Complex of Drosophila." Genetics 199, 17–23. https://doi.org/10.1534/genetics.114.167940

Ahmad, K., 2018. CUT&RUN with Drosophila tissues. https://doi.org/10.17504/protocols.io.umfeu3n

Andersen, P.R., Tirian, L., Vunjak, M., Brennecke, J., 2017. A heterochromatin-dependent transcription machinery drives piRNA expression. Nature. https://doi.org/10.1038/nature23482

Ben-Ami, F., Heller, J., 2005. Spatial and temporal patterns of parthenogenesis and parasitism in the freshwater snail Melanoides tuberculata. Journal of Evolutionary Biology 18, 138–146. https://doi.org/10.1111/j.1420-9101.2004.00791.x

Blatt, P., Martin, E.T., Breznak, S.M., Rangan, P., 2020. Post-transcriptional gene regulation regulates germline stem cell to oocyte transition during Drosophila oogenesis. Curr Top Dev Biol 140, 3–34. https://doi.org/10.1016/bs.ctdb.2019.10.003

Blatt, P., Wong-Deyrup, S.W., McCarthy, A., Breznak, S., Hurton, M.D., Upadhyay, M., Bennink, B., Camacho, J., Lee, M.T., Rangan, P., 2021. RNA degradation is required for the germ-cell to maternal transition in Drosophila. Current Biology 31, 2984-2994.e7. https://doi.org/10.1016/j.cub.2021.04.052

Brickner, D.G., Randise-Hinchliff, C., Lebrun Corbin, M., Liang, J.M., Kim, S., Sump, B., D'Urso, A., Kim, S.H., Satomura, A., Schmit, H., Coukos, R., Hwang, S., Watson, R., Brickner, J.H., 2019. The Role of Transcription Factors and Nuclear Pore Proteins in Controlling the Spatial Organization of the Yeast Genome. Developmental Cell 49, 936-947.e4. https://doi.org/10.1016/j.devcel.2019.05.023

Cahoon, C.K., Hawley, R.S., 2016. Regulating the construction and demolition of the synaptonemal complex, Nature Structural and Molecular Biology. https://doi.org/10.1038/nsmb.3208

Calvi, B.R., Lilly, M.A., Spradling, A.C., 1998. Cell cycle control of chorion gene amplification. Genes Dev 12, 734–744. https://doi.org/10.1101/gad.12.5.734

Capelson, M., Doucet, C., Hetzer, M.W., 2010. Nuclear pore complexes: guardians of the nuclear genome. Cold Spring Harb Symp Quant Biol 75, 585–597. https://doi.org/10.1101/sqb.2010.75.059

Capelson, M., Hetzer, M.W., 2009. The role of nuclear pores in gene regulation, development and disease. EMBO Rep 10, 697–705. https://doi.org/10.1038/embor.2009.147

Capelson, Maya, Liang, Y., Schulte, R., Mair, W., Wagner, U., Hetzer, M.W., 2010. Chromatin-bound nuclear pore components regulate gene expression in higher eukaryotes. Cell 140, 372–383. https://doi.org/10.1016/j.cell.2009.12.054

Carreira-Rosario, A., Bhargava, V., Hillebrand, J., Kollipara, R.K., Ramaswami, M., Buszczak, M., 2016. Repression of Pumilio Protein Expression by Rbfox1 Promotes Germ Cell Differentiation. Developmental Cell 36, 562–571.

Chen, D., McKearin, D., 2003a. Dpp signaling silences bam transcription directly to establish asymmetric divisions of germline stem cells. Current biology : CB 13, 1786–1791.

Chen, D., McKearin, D.M., 2003b. A discrete transcriptional silencer in the bam gene determines asymmetric division of the Drosophila germline stem cell. Development (Cambridge, England) 130, 1159–1170.

Chen, Y., Pane, A., Schüpbach, T., 2007. Cutoff and Aubergine mutations result in upregulation of retrotransposons and activation of a checkpoint in the Drosophila germline. Curr Biol 17, 637–642. https://doi.org/10.1016/j.cub.2007.02.027

1091   Cinalli, R.M., Rangan, P., Lehmann, R., 2008. Germ cells are forever. Cell 132, 559–562.
1092   Clough, E., Moon, W., Wang, S., Smith, K., Hazelrigg, T., 2007. Histone methylation is required
1093   for oogenesis in Drosophila. Development 134, 157–165.
1094   https://doi.org/10.1242/dev.02698
1095   Clough, E., Tedeschi, T., Hazelrigg, T., 2014. Epigenetic regulation of oogenesis and germ stem
1096   cell maintenance by the Drosophila histone methyltransferase Eggless/dSetDB1.
1097   Developmental Biology 388, 181–191. https://doi.org/10.1016/j.ydbio.2014.01.014
1098   Colozza, G., Montembault, E., Quénerch'du, E., Riparbelli, M.G., D'Avino, P.P., Callaini, G.,
1099   2011. Drosophila nucleoporin Nup154 controls cell viability, proliferation and nuclear
1100   accumulation of Mad transcription factor. Tissue and Cell 43, 254–261.
1101   https://doi.org/10.1016/j.tice.2011.05.001
1102   Czech, B., Munafò, M., Ciabrelli, F., Eastwood, E.L., Fabry, M.H., Kneuss, E., Hannon, G.J.,
1103   2018. piRNA-Guided Genome Defense: From Biogenesis to Silencing. Annu Rev Genet
1104   52, 131–157. https://doi.org/10.1146/annurev-genet-120417-031441
1105   Dansereau, D.A., Lasko, P., 2008. The Development of Germline Stem Cells in Drosophila.
1106   Methods Mol Biol 450, 3–26. https://doi.org/10.1007/978-1-60327-214-8_1
1107   Davis, L.I., Blobel, G., 1987. Nuclear pore complex contains a family of glycoproteins that
1108   includes p62: glycosylation through a previously unidentified cellular pathway. PNAS 84,
1109   7552–7556. https://doi.org/10.1073/pnas.84.21.7552
1110   Devlin, R.H., Bingham, B., Wakimoto, B.T., 1990. The organization and expression of the light
1111   gene, a heterochromatic gene of Drosophila melanogaster. Genetics 125, 129–140.
1112   Doucet, C.M., Hetzer, M.W., 2010. Nuclear pore biogenesis into an intact nuclear envelope.
1113   Chromosoma 119, 469–477. https://doi.org/10.1007/s00412-010-0289-2
1114   Duan, T., Green, N., Tootle, T.L., Geyer, P.K., 2020. Nuclear architecture as an intrinsic
1115   regulator of Drosophila female germline stem cell maintenance. Current Opinion in
1116   Insect Science, Development and regulation 37, 30–38.
1117   https://doi.org/10.1016/j.cois.2019.11.007
1118   Eymery, A., Liu, Z., Ozonov, E.A., Stadler, M.B., Peters, A.H.F.M., 2016. The methyltransferase
1119   Setdb1 is essential for meiosis and mitosis in mouse oocytes and early embryos.
1120   Development 143, 2767–2779. https://doi.org/10.1242/dev.132746
1121   Flora, P., McCarthy, A., Upadhyay, M., Rangan, P., 2017. Role of chromatin modifications in
1122   Drosophila germline stem cell differentiation, in: Results and Problems in Cell
1123   Differentiation. pp. 1–30. https://doi.org/10.1007/978-3-319-44820-6_1
1124   Flora, P., Schowalter, S., Wong-Deyrup, S., DeGennaro, M., Nasrallah, M.A., Rangan, P., 2018.
1125   Transient transcriptional silencing alters the cell cycle to promote germline stem cell
1126   differentiation in Drosophila. Developmental biology 434, 84–95.
1127   Frietze, S., O'Geen, H., Blahnik, K.R., Jin, V.X., Farnham, P.J., 2010. ZNF274 Recruits the
1128   Histone Methyltransferase SETDB1 to the 3′ Ends of ZNF Genes. PLOS ONE 5,
1129   e15082. https://doi.org/10.1371/journal.pone.0015082
1130   Gerbasi, V.R., Preall, J.B., Golden, D.E., Powell, D.W., Cummins, T.D., Sontheimer, E.J., 2011.
1131   Blanks, a nuclear siRNA/dsRNA-binding complex component, is required for Drosophila
1132   spermiogenesis. PNAS 108, 3204–3209. https://doi.org/10.1073/pnas.1009781108
1133   Gigliotti, S., Callaini, G., Andone, S., Riparbelli, M.G., Pernas-Alonso, R., Hoffmann, G.,
1134   Graziani, F., Malva, C., 1998. Nup154, a new Drosophila gene essential for male and
1135   female gametogenesis is related to the nup155 vertebrate nucleoporin gene. J Cell Biol
1136   142, 1195–1207. https://doi.org/10.1083/jcb.142.5.1195
1137   Gilboa, L., Lehmann, R., 2004. Repression of primordial germ cell differentiation parallels germ
1138   line stem cell maintenance. Curr Biol 14, 981–986.
1139   https://doi.org/10.1016/j.cub.2004.05.049
1140   Gozalo, A., Capelson, M., 2016. A New Path through the Nuclear Pore. Cell 167, 1159–1160.
1141   https://doi.org/10.1016/j.cell.2016.11.011

Grimaldi, M.R., Cozzolino, L., Malva, C., Graziani, F., Gigliotti, S., 2007. nup154 genetically interacts with cup and plays a cell-type-specific function during Drosophila melanogaster egg-chamber development. Genetics 175, 1751–1759. https://doi.org/10.1534/genetics.106.062844

Güttinger, S., Laurell, E., Kutay, U., 2009. Orchestrating nuclear envelope disassembly and reassembly during mitosis. Nat Rev Mol Cell Biol 10, 178–191. https://doi.org/10.1038/nrm2641

Hampoelz, B., Schwarz, A., Ronchi, P., Bragulat-Teixidor, H., Tischer, C., Gaspar, I., Ephrussi, A., Schwab, Y., Beck, M., 2019. Nuclear Pores Assemble from Nucleoporin Condensates During Oogenesis. Cell 179, 671-686.e17. https://doi.org/10.1016/j.cell.2019.09.022

Holla, S., Dhakshnamoorthy, J., Folco, H.D., Balachandran, V., Xiao, H., Sun, L., Wheeler, D., Zofall, M., Grewal, S.I.S., 2020. Positioning heterochromatin at the nuclear periphery suppresses histone turnover to promote epigenetic inheritance. Cell 180, 150-164.e15. https://doi.org/10.1016/j.cell.2019.12.004

Hou, C., Corces, V.G., 2010. Nups take leave of the nuclear envelope to regulate transcription. Cell 140, 306–308. https://doi.org/10.1016/j.cell.2010.01.036

Hughes, S.E., Miller, D.E., Miller, A.L., Hawley, R.S., 2018. Female Meiosis: Synapsis, Recombination, and Segregation in Drosophila melanogaster. Genetics 208, 875–908. https://doi.org/10.1534/genetics.117.300081

Huynh, J.-R., St Johnston, D., 2004. The Origin of Asymmetry: Early Polarisation of the Drosophila Germline Cyst and Oocyte. Current Biology 14, R438–R449. https://doi.org/10.1016/j.cub.2004.05.040

Iglesias, N., Paulo, J.A., Tatarakis, A., Wang, X., Edwards, A.L., Bhanu, N.V., Garcia, B.A., Haas, W., Gygi, S.P., Moazed, D., 2020. Native Chromatin Proteomics Reveals Role for Specific Nucleoporins in Heterochromatin Organization and Maintenance. Mol Cell 77, 51-66.e8. https://doi.org/10.1016/j.molcel.2019.10.018

Jevitt, A., Chatterjee, D., Xie, G., Wang, X.-F., Otwell, T., Huang, Y.-C., Deng, W.-M., 2020. A single-cell atlas of adult Drosophila ovary identifies transcriptional programs and somatic cell lineage regulating oogenesis. PLOS Biology 18, e3000538. https://doi.org/10.1371/journal.pbio.3000538

Katsani, K.R., Karess, R.E., Dostatni, N., Doye, V., 2008. In Vivo Dynamics of Drosophila Nuclear Envelope Components. MBoC 19, 3652–3666. https://doi.org/10.1091/mbc.e07-11-1162

Kershner, A., Crittenden, S.L., Friend, K., Sorensen, E.B., Porter, D.F., Kimble, J., 2013. Germline Stem Cells and Their Regulation in the Nematode Caenorhabditis elegans, in: Hime, G., Abud, H. (Eds.), Transcriptional and Translational Regulation of Stem Cells, Advances in Experimental Medicine and Biology. Springer Netherlands, Dordrecht, pp. 29–46. https://doi.org/10.1007/978-94-007-6621-1_3

Kiseleva, E., Rutherford, S., Cotter, L.M., Allen, T.D., Goldberg, M.W., 2001. Steps of nuclear pore complex disassembly and reassembly during mitosis in early Drosophila embryos. Journal of Cell Science 114, 3607–3618. https://doi.org/10.1242/jcs.114.20.3607

Ko, K., Araúzo-Bravo, M.J., Kim, J., Stehling, M., Schöler, H.R., 2010. Conversion of adult mouse unipotent germline stem cells into pluripotent stem cells. Nat Protoc 5, 921–928. https://doi.org/10.1038/nprot.2010.44

Koch, C.M., Honemann-Capito, M., Egger-Adam, D., Wodarz, A., 2009. Windei, the Drosophila Homolog of mAM/MCAF1, Is an Essential Cofactor of the H3K9 Methyl Transferase dSETDB1/Eggless in Germ Line Development. PLoS Genet 5, e1000644. https://doi.org/10.1371/journal.pgen.1000644

Koch, E.A., Smith, P.A., King, R.C., 1967. The division and differentiation of Drosophila cystocytes. J. Morphol. 121, 55–70. https://doi.org/10.1002/jmor.1051210106

1193 Kugler, J.-M., Lasko, P., 2009. Localization, anchoring and translational control of oskar,
1194   gurken, bicoid and nanos mRNA during Drosophila oogenesis. Fly (Austin) 3, 15–28.
1195   https://doi.org/10.4161/fly.3.1.7751
1196 Kuhn, T.M., Pascual-Garcia, P., Gozalo, A., Little, S.C., Capelson, M., 2019. Chromatin
1197   targeting of nuclear pore proteins induces chromatin decondensation. Journal of Cell
1198   Biology 218, 2945–2961. https://doi.org/10.1083/jcb.201807139
1199 Kutay, U., Jühlen, R., Antonin, W., 2021. Mitotic disassembly and reassembly of nuclear pore
1200   complexes. Trends in Cell Biology. https://doi.org/10.1016/j.tcb.2021.06.011
1201 Lasko, P.F., Ashburner, M., 1988. The product of the Drosophila gene vasa is very similar to
1202   eukaryotic initiation factor-4A. Nature 335, 611–617. https://doi.org/10.1038/335611a0
1203 Laurell, E., Kutay, U., 2011. Dismantling the NPC permeability barrier at the onset of mitosis.
1204   Cell Cycle 10, 2243–2245. https://doi.org/10.4161/cc.10.14.16195
1205 Lehmann, R., 2012. Germline Stem Cells: Origin and Destiny. Cell Stem Cell 10, 729–739.
1206   https://doi.org/10.1016/j.stem.2012.05.016
1207 Lesch, B.J., Page, D.C., 2012. Genetics of germ cell development. Nature Reviews Genetics.
1208   https://doi.org/10.1038/nrg3294
1209 Lilly, M.A., Spradling, A.C., 1996. The Drosophila endocycle is controlled by Cyclin E and lacks
1210   a checkpoint ensuring S-phase completion. Genes Dev 10, 2514–2526.
1211   https://doi.org/10.1101/gad.10.19.2514
1212 Mach, J.M., Lehmann, R., 1997. An Egalitarian-BicaudalD complex is essential for oocyte
1213   specification and axis determination in Drosophila. Genes Dev. 11, 423–435.
1214   https://doi.org/10.1101/gad.11.4.423
1215 Malone, C.D., Brennecke, J., Dus, M., Stark, A., McCombie, W.R., Sachidanandam, R.,
1216   Hannon, G.J., 2009. Specialized piRNA Pathways Act in Germline and Somatic Tissues
1217   of the Drosophila Ovary. Cell 137, 522–535. https://doi.org/10.1016/j.cell.2009.03.040
1218 McCarthy, A., Sarkar, K., Martin, E.T., Upadhyay, M., James, J.R., Lin, J.M., Jang, S., Williams,
1219   N.D., Forni, P.E., Buszczak, M., Rangan, P., 2019. MSL3 coordinates a transcriptional
1220   and translational meiotic program in female Drosophila. bioRxiv 2019.12.18.879874.
1221   https://doi.org/10.1101/2019.12.18.879874
1222 McCloskey, A., Ibarra, A., Hetzer, M.W., 2018. Tpr regulates the total number of nuclear pore
1223   complexes per cell nucleus. Genes Dev. 32, 1321–1331.
1224   https://doi.org/10.1101/gad.315523.118
1225 McKearin, D., Ohlstein, B., 1995. A role for the Drosophila bag-of-marbles protein in the
1226   differentiation of cystoblasts from germline stem cells. Development (Cambridge,
1227   England) 121, 2937–2947.
1228 McKearin, D.M., Spradling, A.C., 1990. bag-of-marbles: a Drosophila gene required to initiate
1229   both male and female gametogenesis. Genes & development 4, 2242–2251.
1230 Navarro, C., Puthalakath, H., Adams, J.M., Strasser, A., Lehmann, R., 2004. Egalitarian binds
1231   dynein light chain to establish oocyte polarity and maintain oocyte fate. Nat Cell Biol 6,
1232   427–435. https://doi.org/10.1038/ncb1122
1233 Orr-Weaver, T.L., 1995. Meiosis in Drosophila: seeing is believing. Proceedings of the National
1234   Academy of Sciences of the United States of America 92, 10443–10449.
1235 Osumi, K., Sato, K., Murano, K., Siomi, H., Siomi, M.C., 2019. Essential roles of Windei and
1236   nuclear monoubiquitination of Eggless/SETDB1 in transposon silencing. EMBO Rep 20,
1237   e48296. https://doi.org/10.15252/embr.201948296
1238 Page, S.L., Hawley, R.S., 2001. c(3)G encodes a Drosophila synaptonemal complex protein.
1239   Genes & development 15, 3130–3143.
1240 Rangan, P., Malone, C.D., Navarro, C., Newbold, S.P., Hayes, P.S., Sachidanandam, R.,
1241   Hannon, G.J., Lehmann, R., 2011. piRNA production requires heterochromatin formation
1242   in Drosophila. Curr Biol 21, 1373–1379. https://doi.org/10.1016/j.cub.2011.06.057

1243 Reik, W., Surani, M.A., 2015. Germline and Pluripotent Stem Cells. Cold Spring Harb Perspect
1244   Biol 7, a019422. https://doi.org/10.1101/cshperspect.a019422
1245 Riparbelli, M.G., Gottardo, M., Callaini, G., 2017. Parthenogenesis in Insects: The Centriole
1246   Renaissance. Results Probl Cell Differ 63, 435–479. https://doi.org/10.1007/978-3-319-
1247   60855-6_19
1248 Sarma, N.J., Willis, K., 2012. The new nucleoporin: regulator of transcriptional repression and
1249   beyond. Nucleus 3, 508–515. https://doi.org/10.4161/nucl.22427
1250 Schultz, D.C., Ayyanathan, K., Negorev, D., Maul, G.G., Rauscher, F.J., 2002. SETDB1: a novel
1251   KAP-1-associated histone H3, lysine 9-specific methyltransferase that contributes to
1252   HP1-mediated silencing of euchromatic genes by KRAB zinc-finger proteins. Genes Dev
1253   16, 919–932. https://doi.org/10.1101/gad.973302
1254 Schwartz, Y.B., Cavalli, G., 2017. Three-Dimensional Genome Organization and Function in
1255   Drosophila. Genetics 205, 5–24. https://doi.org/10.1534/genetics.115.185132
1256 Seum, C., Reo, E., Peng, H., Rauscher, F.J., Spierer, P., Bontron, S., 2007. Drosophila
1257   SETDB1 Is Required for Chromosome 4 Silencing. PLoS Genet 3, e76.
1258   https://doi.org/10.1371/journal.pgen.0030076
1259 Seydoux, G., Braun, R.E., 2006. Pathway to totipotency: lessons from germ cells. Cell 127,
1260   891–904. https://doi.org/10.1016/j.cell.2006.11.016
1261 Shapiro-Kulnane, L., Smolko, A.E., Salz, H.K., 2015. Maintenance of Drosophila germline stem
1262   cell sexual identity in oogenesis and tumorigenesis. Development 142, 1073–1082.
1263   https://doi.org/10.1242/dev.116590
1264 Sienski, G., Dönertas, D., Brennecke, J., 2012. Transcriptional Silencing of Transposons by Piwi
1265   and Maelstrom and Its Impact on Chromatin State and Gene Expression. Cell 151, 964–
1266   980. https://doi.org/10.1016/j.cell.2012.10.040
1267 Skene, P.J., Henikoff, S., 2017. An efficient targeted nuclease strategy for high-resolution
1268   mapping of DNA binding sites. eLife 6, e21856. https://doi.org/10.7554/eLife.21856
1269 Smolko, A.E., Shapiro-Kulnane, L., Salz, H.K., 2020. An autoregulatory switch in sex-specific
1270   phf7 transcription causes loss of sexual identity and tumors in the Drosophila female
1271   germline. Development 147. https://doi.org/10.1242/dev.192856
1272 Smolko, A.E., Shapiro-Kulnane, L., Salz, H.K., 2018. The H3K9 methyltransferase SETDB1
1273   maintains female identity in Drosophila germ cells. Nat Commun 9, 4155.
1274   https://doi.org/10.1038/s41467-018-06697-x
1275 Sood, V., Brickner, J.H., 2014. Nuclear pore interactions with the genome. Curr Opin Genet Dev
1276   25, 43–49. https://doi.org/10.1016/j.gde.2013.11.018
1277 Spradling, A., Fuller, M.T., Braun, R.E., Yoshida, S., 2011. Germline Stem Cells. Cold Spring
1278   Harb Perspect Biol 3, a002642. https://doi.org/10.1101/cshperspect.a002642
1279 Spradling, Allan C, 1993. Developmental genetics of oogenesis, in: The Development of
1280   Drosophila Melanogaster.
1281 Spradling, A C, 1993. Germline cysts: communes that work. Cell 72, 649–651.
1282 Telfer, W.H., 1975. Development and Physiology of the Oöcyte-Nurse Cell Syncytium.
1283   Advances in Insect Physiology. https://doi.org/10.1016/S0065-2806(08)60164-2
1284 Timms, R.T., Tchasovnikarova, I.A., Antrobus, R., Dougan, G., Lehner, P.J., 2016. ATF7IP-
1285   Mediated Stabilization of the Histone Methyltransferase SETDB1 Is Essential for
1286   Heterochromatin Formation by the HUSH Complex. Cell Rep 17, 653–659.
1287   https://doi.org/10.1016/j.celrep.2016.09.050
1288 Tsusaka, T., Shimura, C., Shinkai, Y., 2019. ATF7IP regulates SETDB1 nuclear localization and
1289   increases its ubiquitination. EMBO Rep 20, e48297.
1290   https://doi.org/10.15252/embr.201948297
1291 Upadhyay, M., Martino Cortez, Y., Wong-Deyrup, S., Tavares, L., Schowalter, S., Flora, P., Hill,
1292   C., Nasrallah, M.A., Chittur, S., Rangan, P., 2016. Transposon Dysregulation Modulates

1293   dWnt4 Signaling to Control Germline Stem Cell Differentiation in Drosophila. PLoS
1294   genetics 12, e1005918.
1295 Valm, A.M., Cohen, S., Legant, W.R., Melunis, J., Hershberg, U., Wait, E., Cohen, A.R.,
1296   Davidson, M.W., Betzig, E., Lippincott-Schwartz, J., 2017. Applying systems-level
1297   spectral imaging and analysis to reveal the organelle interactome. Nature 546, 162–167.
1298   https://doi.org/10.1038/nature22369
1299 Wang, W., Han, B.W., Tipping, C., Ge, D.T., Zhang, Z., Weng, Z., Zamore, P.D., 2015. Slicing
1300   and Binding by Ago3 or Aub Trigger Piwi-Bound piRNA Production by Distinct
1301   Mechanisms. Mol Cell 59, 819–830. https://doi.org/10.1016/j.molcel.2015.08.007
1302 Weiler, K.S., Wakimoto, B.T., 1995. Heterochromatin and gene expression in Drosophila. Annu
1303   Rev Genet 29, 577–605. https://doi.org/10.1146/annurev.ge.29.120195.003045
1304 Wilson, J.E., Connell, J.E., Macdonald, P.M., 1996. aubergine enhances oskar translation in the
1305   Drosophila ovary. Development 122, 1631–1639. https://doi.org/10.1242/dev.122.5.1631
1306 Xie, T., 2013. Control of germline stem cell self-renewal and differentiation in the Drosophila
1307   ovary: concerted actions of niche signals and intrinsic factors. Wiley Interdiscip Rev Dev
1308   Biol 2, 261–273. https://doi.org/10.1002/wdev.60
1309 Xie, T., Spradling, A.C., 2000. A niche maintaining germ line stem cells in the Drosophila ovary.
1310   Science 290, 328–330. https://doi.org/10.1126/science.290.5490.328
1311 Yoon, J., Lee, K.-S., Park, J.S., Yu, K., Paik, S.-G., Kang, Y.-K., 2008. dSETDB1 and
1312   SU(VAR)3–9 Sequentially Function during Germline-Stem Cell Differentiation in
1313   Drosophila melanogaster. PLOS ONE 3, e2234.
1314   https://doi.org/10.1371/journal.pone.0002234
1315 Yuan, H., Yamashita, Y.M., 2010. Germline stem cells: stems of the next generation. Curr Opin
1316   Cell Biol 22, 730–736. https://doi.org/10.1016/j.ceb.2010.08.013
1317 Zaccai, M., Lipshitz, H.D., 1996. Differential distributions of two adducin-like protein isoforms in
1318   the Drosophila ovary and early embryo. Zygote 4, 159–166.
1319   https://doi.org/10.1017/s096719940000304x
1320